UNIVERSITÉ DE MONTRÉAL

REPRESENTATION OF TYPE 4 WIND TURBINE GENERATOR FOR STEADY STATE SHORT-CIRCUIT CALCULATIONS

WOULÈYE KAMARA

DÉPARTEMENT DE GÉNIE ÉLECTRIQUE

ÉCOLE POLYTECHNIQUE DE MONTRÉAL

MÉMOIRE PRÉSENTÉ EN VUE DE L'OBTENTION

DU DIPLÔME DE MAÎTRISE ÈS SCIENCES APPLIQUÉES

(GÉNIE ÉLECTRIQUE)

DÉCEMBRE 2013

© Woulèye Kamara, 2013.

UNIVERSITÉ DE MONTRÉAL

ÉCOLE POLYTECHNIQUE DE MONTRÉAL

Ce mémoire intitulé:

REPRESENTATION OF TYPE 4 WIND TURBINE GENERATOR FOR STEADY STATE SHORT-CIRCUIT CALCULATIONS

présenté par : KAMARA Woulèye

en vue de l'obtention du diplôme de : Maîtrise ès sciences appliquées

a été dûment accepté par le jury d'examen constitué de :

M. SAYDY Lahcen, Ph.D., président

M. MAHSEREDJIAN Jean, Ph.D., membre et directeur de recherche

M. SOUMARÉ Saidou, M.Sc.A., membre et codirecteur de recherche

M. KOCAR Ilhan, Ph.D., membre

ACKNOWLEDGEMENTS

I would like to express my gratitude to all the people who contributed to any extent to the fulfillment of this master thesis.

First, I would like to thank my research director, Professor Jean Mahseredjian for his valuable guidance and constant support. He has early believed in the benefits of this research project and has encouraged me since then.

I also wish to thank to my co-director and colleague, Saidou Soumare, for proposing this research topic and for his constant support in the realization of this research project. His advices and encouragements have contributed to the fulfillment of this project.

I would like to specially thank my manager, Marc Coursol, General Director of CYME International T&D, for the support that he has provided me throughout these years, for his guidance and for always encouraging me to undertake new challenges.

I am very grateful to my colleagues, Assane Gueye, Jean Sébastien Lacroix, Patrick Jacques. This research wouldn't have been the same without their valuable contribution and feedback.

I am dedicating this work to my parents Nafissatou and Sadibou Kamara, and to my sister, Khadijatou Kamara who have never stopped believing in me, and have provided me endless love and support.

RÉSUMÉ

Plusieurs impacts techniques sont associés à l'interconnexion des éoliennes au réseau électrique. Parmi eux, l'augmentation du niveau de court-circuit du réseau ainsi que son impact sur la coordination de protection a longtemps représenté un frein majeur à l'interconnexion de nouvelles centrales éoliennes au réseau, particulièrement pour les réseaux à moyenne tension [1].

Compte tenu de l'intérêt grandissant pour les énergies renouvelables, les logiciels de calcul de court-circuit utilisés à des fins de planification doivent permettre de mieux évaluer l'impact des centrales éoliennes sur le niveau de court-circuit du réseau auquel elles sont connectées. Malheureusement, très peu ont développé des modèles d'éoliennes à couplage électronique direct dans le domaine fréquentiel qui estiment adéquatement leur contribution au courant de défaut.

La principale contribution de ce travail de recherche est le développement d'un modèle simple et précis d'éolienne à couplage électronique direct pour les calculs de court-circuit en régime permanent. Le modèle développé reproduit le comportement réel de l'éolienne en cas de défaut en modélisant adéquatement l'effet du convertisseur. Les données utilisées pour le modèle sont facilement accessibles aux ingénieurs de planification.

L'autre contribution de ce travail de recherche est le développement d'un algorithme de court-circuit adapté pour prendre en charge le modèle d'éoliennes à couplage électronique direct proposé. Un algorithme de court-circuit basé sur l'analyse-nodale-augmentée modifiée (MANA) est résolu de manière itérative. L'algorithme est implémenté avec succès dans CYME, un logiciel commercial d'analyse des réseaux. Il permet de reproduire la contribution de l'éolienne au courant de défaut du réseau, y compris pour des réseaux complexes et débalancés.

L'étude détaillée du comportement d'une éolienne à couplage électronique direct à l'aide du logiciel de transitoire électromagnétique EMTP-RV démontre que le modèle proposé reproduit fidèlement le comportement réel de l'éolienne en court-circuit.

Le modèle proposé est ensuite implémenté dans le logiciel CYME 7.0 et validé pour différents scénarios en utilisant le réseau de distribution 25 kV de Fortis Alberta. La contribution au courant de défaut obtenue à partir du modèle proposé est comparée à celle obtenue à partir des modèles actuels de CYME.

La validation montre que le modèle proposé permet de déterminer le courant de défaut de l’éolienne à couplage électronique direct avec une meilleure précision que les modèles actuels de CYME 7.0. En outre, la performance et la robustesse de l'algorithme de court-circuit développé permettent d’analyser de grands réseaux débalancés, qui intègrent des éoliennes à couplage électronique direct.

ABSTRACT

Various technical impacts are associated to the interconnection of wind turbine generators to the grid. Among them, the increase of short-circuit levels along with its effect on the settings of protecting relays has long acted as an important inhibiting factor for the interconnection of new wind power plants to the grid. This is especially true at the medium voltage level where networks operate close to their short-circuit design value [1]. As renewable energies are progressively replacing traditional power generation sources, short-circuit studies need to adequately assess the impact of newly interconnected wind power plants on the fault level of the network.

For planning and design purposes, short-circuit studies are usually performed using steady-state short-circuit programs. Unfortunately, very few have developed models of wind turbine generators that accurately estimate their fault contribution in the phase domain. In particular, no commercial fault-flow analysis program specifically addresses the modeling of inverter-based wind turbine generators which behavior is based on the inverter's characteristics rather than the generator's.

The main contribution of this research work is the development of a simplified and yet accurate model of full-scale converter based wind turbine generator, also called Type 4 wind turbine generator, for steady-state short-circuit calculations. The model reproduces the real behavior of the Type 4 wind turbine generator under fault conditions by correctly accounting for the effect of the full-scale converter. The data used for the model is easily accessible to planning engineers. An additional contribution of this research work is the development of a short-circuit algorithm adapted to support the proposed model of Type 4 wind-turbine generator. Short-circuit algorithm based on modified-augmented-nodal analysis (MANA) is solved iteratively to accommodate the proposed model. The algorithm is successfully implemented in CYME 7.0, a commercial distribution system analysis program, to perform short-circuit calculations in multiphase complex unbalanced systems.

Detailed study of the behavior of Type 4 wind turbine generator using electromagnetic type programs like EMTP-RV has assessed that the proposed model closely reproduces the real behavior of the wind turbine generator under steady-state fault conditions. The proposed model is then implemented in CYME 7.0 and validated for different fault scenarios using the Fortis Alberta 25 kV distribution system as benchmark. The fault contribution obtained from the

proposed model is compared against the one obtained from the previous model implemented in CYME 7.0. The validation test cases show that the proposed model estimates the fault contribution of the wind turbine generator with better precision than the former models. Besides, the performance and robustness of the short-circuit algorithm developed allow handling unbalanced networks with inverter interfaced wind turbine generators as it is based on the MANA formulation.

TABLE OF CONTENTS

ACKNOWLEDGEMENTS III

RÉSUMÉ IV

ABSTRACT VI

TABLE OF CONTENTS VIII

LIST OF TABLES XI

LIST OF FIGURES XII

LIST OF NOTATIONS AND ABBREVIATIONS XIV

CHAPITRE 1 INTRODUCTION 1

1.1 Background 1

1.2 Problem definition 2

1.3 Objective and methodology 2

1.3.1 Objective 2

1.3.2 Methodology 3

1.4 Report outline 3

1.5 Original contribution 4

CHAPITRE 2 DESCRIPTION OF TYPE 4 WTG 5

2.1 Principles of energy conversion 5

2.2 Wind turbine control philosophies 7

2.2.1 Passive stall control 7

2.2.2 Pitch control 8

2.3 Generator-converter description 8

2.4 Fault-ride through 9

2.4.1 Low voltage ride-through requirements 10

2.4.2 Active power restoration 13

2.4.3 Reactive current injection for voltage support 13

CHAPITRE 3 DETAILED STUDY OF TYPE 4 WTG UNDER FAULT CONDITIONS 15

3.1 Description of the study network 15

3.2 Fault contribution of Type 4 WTG under various fault conditions 17

3.2.1 Three-phase fault (LLL) 17

3.2.2 Single line-to-ground fault (LG) 21

CHAPITRE 4 SHORT-CIRCUIT ANALYSIS IN NETWORKS WITH TYPE 4 WTG 25

4.1 Purpose of short-circuit studies 25

4.2 Literature review 26

CHAPITRE 5 SHORT-CIRCUIT MANA MODEL FOR TYPE 4 WTG 32

5.1 Newton MANA method 33

5.2 Sub-transient model 37

5.2.1 Controlled generator model 37

5.2.2 Current limiting constraint 41

5.3 Transient model 43

5.4 Short-circuit algorithm 47

5.4.1 Short-circuit calculation methods 47

5.4.2 MANA shunt fault models 48

5.4.3 Fault flow algorithm 51

CHAPITRE 6 MODEL VALIDATION 58

6.1 Validation of the new model against detailed EMTP model 58

6.1.1 Description of the study network 58

6.1.2 Results and discussion 59

6.2 Comparison of the new model with the models in CYME 7.0 62

6.2.1 Description of the study network 62

6.3 Fault contribution of Type 4 WTG under various fault conditions 63

6.3.1 Three-phase fault at various locations 63

6.3.2 Line-to-ground fault at various locations 66

CONCLUSION 69

LIST OF TABLES

Table 3-1 - Transmission line data 16

LIST OF FIGURES

Figure 2-1 : C_p coefficient as a function of λ and pitch angle in degrees [5]. 6

Figure 2-2 : Topology of Type 4 wind turbine generator [5] 9

Figure 2-3 : Minimum FRT requirements according to the E.ON grid code [10] 11

Figure 2-4 : Minimum FRT requirements according to Hydro-Québec grid code [32] 12

Figure 2-5 : Reactive current injection according to the German grid code [9]. 14

Figure 3-1 : Single-line diagram of the benchmark network 15

Figure 3-2 : Voltage at HV-AVM bus (PCC) for a LLL fault 18

Figure 3-3 : Fault current of the FCG (measured at the HV-AVM bus) for a LLL fault 18

Figure 3-4 : VSC current in the dq0 frame for a LLL fault 19

Figure 3-5 : Sequence currents of the FCG (at the HV-AVM bus) for a LLL fault 19

Figure 3-6 : Fault current of the FCG (at the LV side of its transformer) for a LLL fault 20

Figure 3-7 : Sequence currents of the FCG (at the LV side of its transformer) for a LLL fault 21

Figure 3-8 : Voltage at HV-AVM bus (PCC) for a LG fault 21

Figure 3-9: Fault current of the FCG (measured at the HV-AVM bus) for a LG fault 22

Figure 3-10 : VSC current in the dq0 frame for a LG fault 22

Figure 3-11 : Sequence currents of the FCG (measured at the HV-AVM bus) for a LG fault 23

Figure 3-12 : Fault current of the FCG (at the LV side of its transformer) for a LG fault 24

Figure 3-13 : Sequence currents of the FCG (at the LV side of its transformer) for a LG fault 24

Figure 4-1 : Full converter based WTG model in CYME 7.0 30

Figure 5-1 : Reactive current injection according to the German code [10]. 44

Figure 5-2 : Shunt Fault Representation with Impedance [33] 49

Figure 5-3 : MANA LG Fault Model 49

Figure 5-4 : MANA LLL Fault Model [33] 50

Figure 5-5 : Initialization of the fault-flow algorithm. 54

Figure 5-6 : Fault-flow algorithm.....56

Figure 5-7 : Algorithm to check the WTG maximum fault contribution. 57

Figure 6-1: Single-line diagram of the benchmark network 58

Figure 6-2 : Fault contribution of the FCG for a LG fault 59

Figure 6-3 : Fault contribution of the FCG for a LG fault 61

Figure 6-4: Equivalent representation of Fortis Alberta 25 kV distribution system. 62

Figure 6-5: Fault contribution of Type 4 WTG for LLL fault – Pdes = 436.5 kW.....64

Figure 6-6 : Fault contribution of Type 4 WTG for LLL fault – Pdes = 150 kW.....66

Figure 6-7 : Fault contribution of Type 4 WTG for LG fault – Pdes = 436.5 kW.....67

Figure 6-8 : Fault contribution of Type 4 WTG for LG fault – Pdes = 150 kW.....68

LIST OF NOTATIONS AND ABBREVIATIONS

FCG	Full converter generator
FRT	Fault ride-through
HV	High voltage
LRT	Low voltage ride-through
MANA	Modified augmented nodal analysis
MV	Medium voltage
PCC	Point of common coupling
PWM	Pulse width modulation
VSC	Voltage source converter
WT	Wind turbine
WTG	Wind turbine generator

CHAPITRE 1 INTRODUCTION

This thesis presents a new model of full converter based wind generator for steady-state short-circuit calculations. This chapter brings light to the reasons that motivated the need to develop models of full converter based wind turbine generators, also named Type 4 WTG. It describes the objectives of this research work and the methodology used to achieve them. The chapter also provides a report outline and emphasizes the original contribution of the research work.

1.1 Background

Short-circuit studies are important to assess the impact of newly interconnected wind power plants on the fault level of the system. When extending the generating capabilities of existing networks, it is not uncommon that utilities worldwide choose to interconnect wind power plants to an existing network since the price of oil has become unsustainable and the interest in renewable energies is consistently increasing. Throughout the last decades, power utilities have shown a major interest in distributed resources like wind power, solar panels, fuel cells, etc.

Among these resources, wind power stands out as the fastest growing source of renewable energy worldwide with an average growth rate of 25.7% in ten years [14]. Actually, the penetration level of wind energy conversion systems (WECS) has reached a point where it is important to assess their impact on electrical networks. Their fault contribution has long been ignored since wind turbine generators were supposed to disconnect after a fault. However, with the increased penetration level of wind power, utilities are forced to revise their grid code requirements and wind generators are now expected to support the grid voltage during a fault. For this reason, their contribution to the fault level of the network can no longer be disregarded.

Therefore, in order to keep guarantying the safe and reliable operation of networks dominated with grid-connected inverters, power analysis programs should closely reproduce the real behavior of wind turbines, especially during abnormal operating conditions.

1.2 Problem definition

Electromagnetic Transient type programs like EMTP-RV [2] already provide accurate models of WECS to estimate their contribution under abnormal conditions. However, these models are fairly complex and require data which may not be accessible to distribution and planning engineers. In particular, details of the inverter are often held closely by manufacturer. The same is true for stability-type programs like CYMSTAB [42]. As a consequence, steady-state short-circuit programs are widely used to perform short-circuit studies of electrical networks.

Steady-state short-circuit programs are based on standards, namely IEC 60909 [3] and IEEE C37.010 [12], IEEE C37.5 [4], etc.., when it comes to modeling equipment for short-circuit analysis purposes. Although the analytical equations provided by the actual standards have been revised to cover the modeling of most representative distributed generation sources, they still do not include the fault contribution of electronically coupled wind turbine generators with adequate accuracy. In the literature as well ([21], [24], [25]), few models accurately reproduce the effect of the grid side converter on the fault contribution of the wind generator. Most of these models also ignore the fault ride-through requirements of wind generators which, in many national grid codes, have become essential to effectively assess their fault contribution. With the fast progress of grid-connected inverter based generators, it is therefore clear that the need to model them accurately is crucial to better assess their contribution to the short-circuit level of electrical networks.

1.3 Objective and methodology

1.3.1 Objective

The purpose of this research work is to develop a simplified model of full converter based wind turbine generator for steady-state short-circuit analysis. The proposed model should accurately account for the effect of the grid side converter and use data easily accessible to planning engineers. Moreover, it should be sensitive to applicable fault ride through requirements. Finally, traditional short-circuit algorithms must be adapted to support the proposed model of wind turbine generator and closely reproduce its fault current contribution under steady-state abnormal operating conditions. In this research work, the modeling of the DFIG has not been addressed since the current models in CYME 7.0 are adequate enough and correctly represent the crowbar protection.

1.3.2 Methodology

To achieve the objectives previously set, an exhaustive literature review of the methodologies available to represent a full converter based wind turbine generator under steady-state fault conditions, is carried out first. Then, a detailed analysis of the Type 4 WTG under fault conditions is performed using the detailed models in the electromagnetic type program EMTP-RV. Based on the observed behavior, a simplified model of full converter based wind turbine generator is developed, accounting for the effect of the grid side converter. In accordance with the objectives set, the model uses accessible data and allows estimating the fault contribution of the wind generator in accordance with the fault ride through requirements set by applicable grid codes. The proposed model also accounts for the control strategy applied to the wind turbine generator prior to the fault. The model developed is afterwards adapted to an iterative short-circuit calculations algorithm based on the modified-augmented-nodal analysis (MANA) approach [28]. Finally, the model is validated for different fault scenarios using the Fortis Alberta 25 kV distribution system as benchmark. Results obtained are validated against the results provided by the former models developed in CYME 7.0. Validation test cases assess that the model and algorithm developed closely reproduce the fault contribution of the Type 4 WTG during fault conditions.

1.4 Report outline

The present thesis is organized into six chapters.

Chapter 1 introduces the reasons that motivated the need to accurately assess the fault contribution of a full converter based wind generator. It also describes the objectives of the research work along with the methodology used to achieve them.

Chapter 2 describes in details the components of a Type 4 WTG. It also reviews the FRT requirements specific to national grid codes.

Chapter 3 assesses the behavior of a Type 4 WTG under fault conditions through an extensive analysis performed using the detailed models implemented in EMTP-RV.

Chapter 4 explains the purpose of short-circuit studies and reviews the different models of Type 4 WTG proposed in literature, highlighting their scopes and limitations.

Chapter 5 presents the model of Type 4 WTG and the algorithm developed to estimate the steady-state fault contribution of a wind turbine generator. Effect of fault ride-through requirements and pre-fault control strategies are also taken into account in the proposed model.

Chapter 6 presents the test cases used to validate the proposed model and algorithm along with the results of the comparison performed between the proposed model and the models implemented in CYME 7.0, a commercial program for distribution networks analysis.

1.5 Original contribution

The main contribution of this research work is the development of accurate but yet simple models of Type 4 WTG for steady-state short-circuit calculations. The modelaccounts for the pre-fault control operating set-points and the applicable fault ride through requirements. Hence, it accurately reproduces the effect of the grid side converter on the generator's fault current contribution. The other main contribution of this research work consists in adapting a MANA based algorithm presented in [28] to support the proposed model of Type 4 WTG for short-circuit analysis and accurately assess the impact of these types of generators on the fault current level of networks to which they are connected.

CHAPITRE 2 DESCRIPTION OF TYPE 4 WTG

2.1 Principles of energy conversion

The wind turbine converts the kinetic energy of the wind into mechanical power which is represented by equation (2.1):

$$P_w = \frac{\rho}{2}\pi r^2 V_w^3 C_p \tag{2.1}$$

where:

ρ : Air density.

r : Blade radius.

V_w : Wind speed.

C_p : Performance coefficient.

Equation (2.1)shows that the mechanical power extracted from the wind turbine varies according to the cube of the wind speed. Therefore, it would be legitimate to expect that the strongest the wind, the more power can be extracted from the wind turbine. In practice however, wind turbines are started at a cut-in wind speed above 5 m/s and they are designed to support winds between 10 to 15 m/s [5]. They are generally stopped at cut-out wind speed, which are lower than gusts winds, for which the wind turbine is at risk of being damaged.

Due to the intermittent nature of the wind and the narrow speed range at which the FCG can operate, equation (2.1) suggests that another parameter that can be controlled to maximize the mechanical power extracted from the wind turbine is its performance coefficient, C_p, which is function of the tip-speed ratio and the blade pitch angle. The tip-speed ratio, λ, is defined as:

$$\lambda = \frac{r\Omega_t}{V_w} \tag{2.2}$$

where:

Ω_t : Turbine rotational speed.

As for the blade pitch angle, it can be controlled through different strategies described hereafter. Provided that the turbine rotational speed and the pitch angle are kept constant, Figure 2-1taken from [5], shows that the performance coefficient is optimal for a narrow range of wind speeds, above which, Cp decreases as the tip-speed ratio increases.

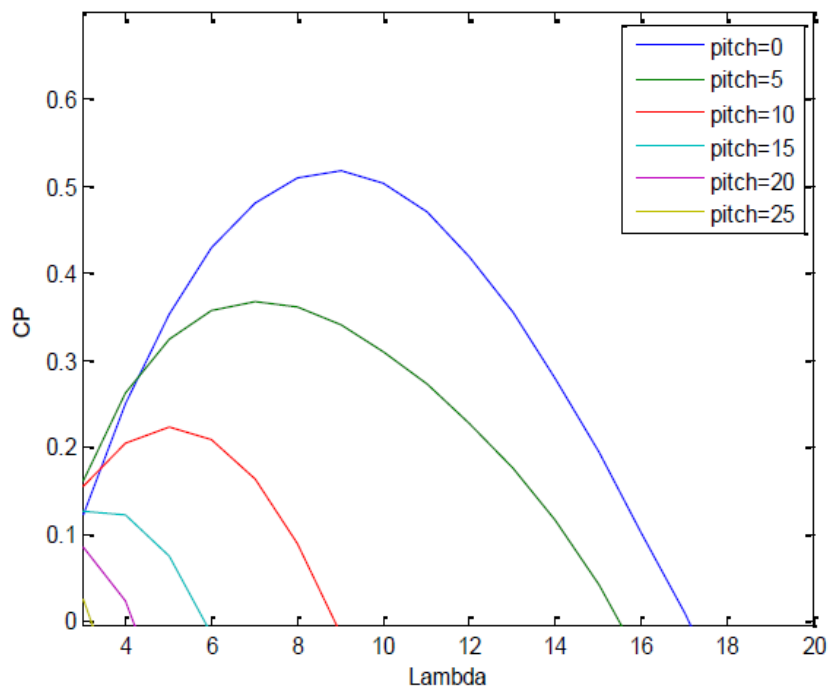

Figure 2-1 : C_p coefficient as a function of λ and pitch angle in degrees [5].

Figure 2-1 also shows that, at constant tip-speed ratio, C_p increases as the pitch angle decreases. Since, unlike the wind speed, the pitch angle can be controlled, it is used to optimize the performance coefficient of the wind turbine, hence, maximizing the mechanical power extracted from the wind turbine regardless of the wind speed available.

Theoretically, due to the effect of the wind turbine on the wind velocity, wind turbines can capture at most 59% of the wind power available. This is called the Betz's limit [43]. In practice however, only 40 to 50% of the wind power is extracted by current wind turbines.

2.2 Wind turbine control philosophies

For a given wind speed, it is clear from equation (2.1) that the only parameter that allows controlling the power extracted from the wind turbine is the performance coefficient C_p. Based on this principle, various active or passive control strategies are developed in order to optimize the power extracted from the wind turbine at given wind speeds.

In particular, at high wind speeds (before the cut-out speed), wind turbines employ these control strategies to waste part of the excess energy of the wind in order to keep producing energy without damaging the turbine.

The main control strategies currently used for power regulation are described hereafter.

2.2.1 Passive stall control

The blades of passive stall controlled wind turbines are aerodynamically designed to produce turbulence beyond a specific wind speed, gradually increasing the angle of attack of the blades until leading the blades to stall. At high wind speeds, this mechanism allows limiting the mechanical power produced by the wind turbine to protect it from possible damages without the need for active controls. In this type of control, the pitch angle is fixed, hence the low maintenance cost associated to less mechanically moving elements compared to pitch regulated wind turbines. However, the drawback of this power regulation strategy is that, above nominal wind speed, it leads to a drop below nominal power. Besides, a significant disadvantage of stall-regulated wind turbines is the voltage flicker produced as a result of the sensitivity of the turbine torque to any slight change in the wind speed. This is true especially when the wind turbine is connected to a weak power system [5].

2.2.2 Pitch control

Pitch controlled wind turbines are equipped with a closed-loop rotor speed controller which regulates the pitch angle of the rotor blades to optimize the mechanical power delivered by the wind turbine according to the wind speed variations [6]. As a result, depending on the wind speed, the rotor blades are either pitched toward the wind to maximize the wind energy capture or turned out of the wind to protect the wind turbine from excessive mechanical stress. During normal operation for which the wind speed ranges from start-up to nominal wind speed, the pitch angle is adjusted to optimize Cp, thus, optimize the power output of the turbine. At high winds, unlike stall controlled wind turbines for which the power output drops with wind speed, the blades of pitch regulated wind turbines are adjusted to allow maintaining a constant nominal power output [5].

2.3 Generator-converter description

A type 4 WTG is composed of a variable-speed wind turbine generator which stator is connected to the grid via a full scale back-to-back converter. A permanent magnet generator is generally used in this type of configuration. However, a wound rotor generator or an induction generator can be used as well.

The full scale frequency converter is composed of back-to-back voltage source converters: an AC-to-DC rectifier and a DC-to-AC inverter. It allows operating the wind turbine within a wide range of frequencies which vary according to the prevailing wind conditions. In particular, the purpose of the grid-side converter is not only to convert the operating frequency of the WTG to the grid frequency but also to decouple the grid from the WTG. Hence, during grid disturbances, the mechanical dynamic of the WTG is isolated from the grid transient dynamic [17], allowing more effective management of mechanical loads [26].

The power converter allows controlling the real and reactive powers independently, within the margin of the maximum converter's current. In practice, the power converter is designed with an overload capability of 10% above rated current [17]. The active power control allows optimizing the performance of the WTG for various prevailing wind conditions whereas the reactive power control is used for voltage regulation at the PCC or at a more distant node [10], [17].

The Type 4 WTG offers great flexibility for LVRT control, voltage regulation and reactive power control [5].

The topology of a Type 4 WTG is shown in Figure 2-1.

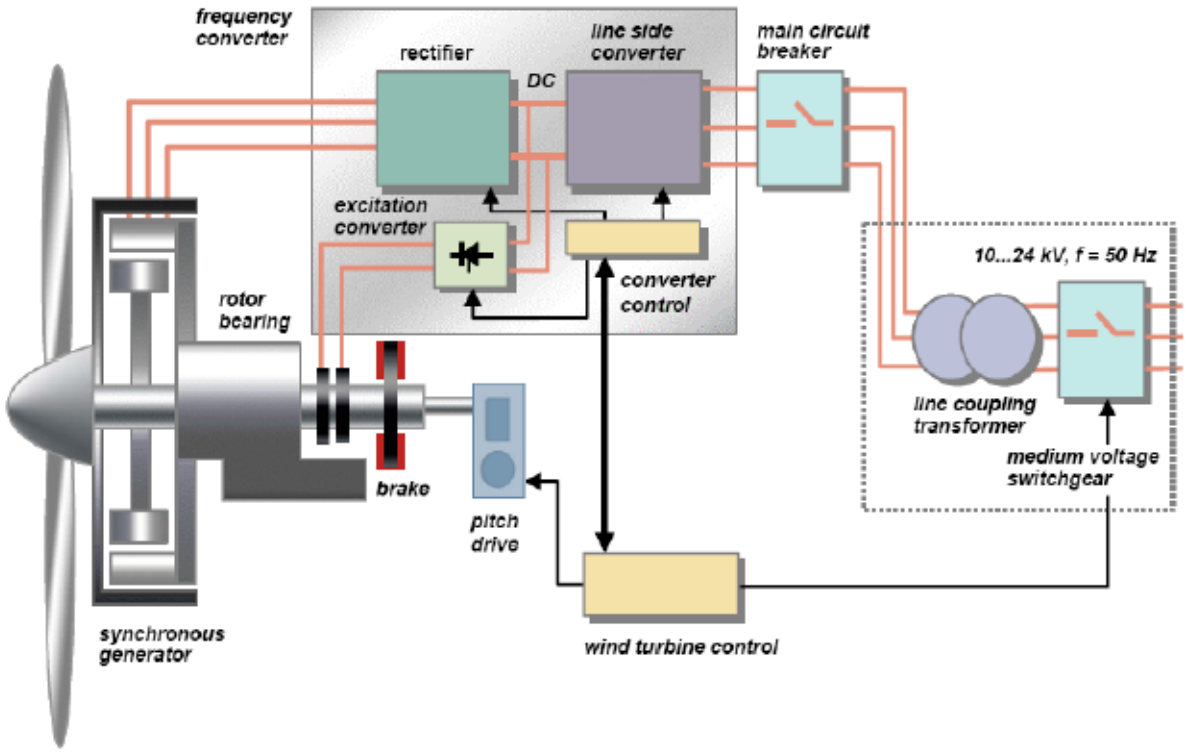

Figure 2-2 : Topology of Type 4 wind turbine generator [5]

2.4 Fault-ride through

In the past couple of years, the fast progress in wind power technology has contributed to improving its competitiveness to levels comparable with conventional power generation methods [9]. As wind technology has become a very attractive solution in terms of cost and environmental impact, several countries are planning to gradually replace the conventional power plants by wind power plants over the coming years [40]. The growth in installed wind power capacity has led the transmission system operators (TSOs) to update the applicable grid codes with technical requirements specific to the connection of large wind farms. Based on the TSOs' accumulated experience, the technical challenges that need to be addressed mainly concern the impact of wind

power plants on grid stability, power quality and their behavior during fault situations. In the latter case, grid codes require wind power plants to remain connected during and after a fault to ensure fast restoration of the active power to the pre-fault levels right after fault clearance [10]. Besides, in countries with high wind power penetration levels, wind farms are expected to contribute to power system voltage and frequency control like conventional power plants [10]. As a result, many new grid codes require the wind turbine to inject reactive current into the grid to provide voltage support during grid disturbances and avoid the loss of stability in networks [37], [39], [32].

This section will provide a brief review of the common grid code requirements developed for wind power plants interconnection to the grid in Germany and in Canada as they are among the most demanding. For the purpose of this dissertation, we will limit our discussion to the requirements related to the behavior of wind turbines during fault situations, that is to say the requirements in terms of fault ride-through capability, active power regulation as well as voltage regulation capabilities.

2.4.1 Low voltage ride-through requirements

Depending on the type and location of the fault affecting the grid, various buses may be affected by voltage dips or voltage rises in one or more phases. LVRT requirements, also known as fault-ride-through (FRT) requirements refer to the ability of wind turbines to remain connected to the grid for a specified duration while withstanding voltage dips down to a given percentage of the nominal voltage [9], [10]. This capability is defined as a voltage against time characteristic which indicates the minimum voltage dips that the wind turbine should withstand without disconnecting from the grid.

As shown in Figure 2-3 and Figure 2-4, the FRT curve varies depending on the protection philosophy and the power system characteristics specific to each country or region. Besides, depending on the grid code, the prescribed voltage dip may either be symmetric or correspond to the maximum voltage drop of all phases [10].

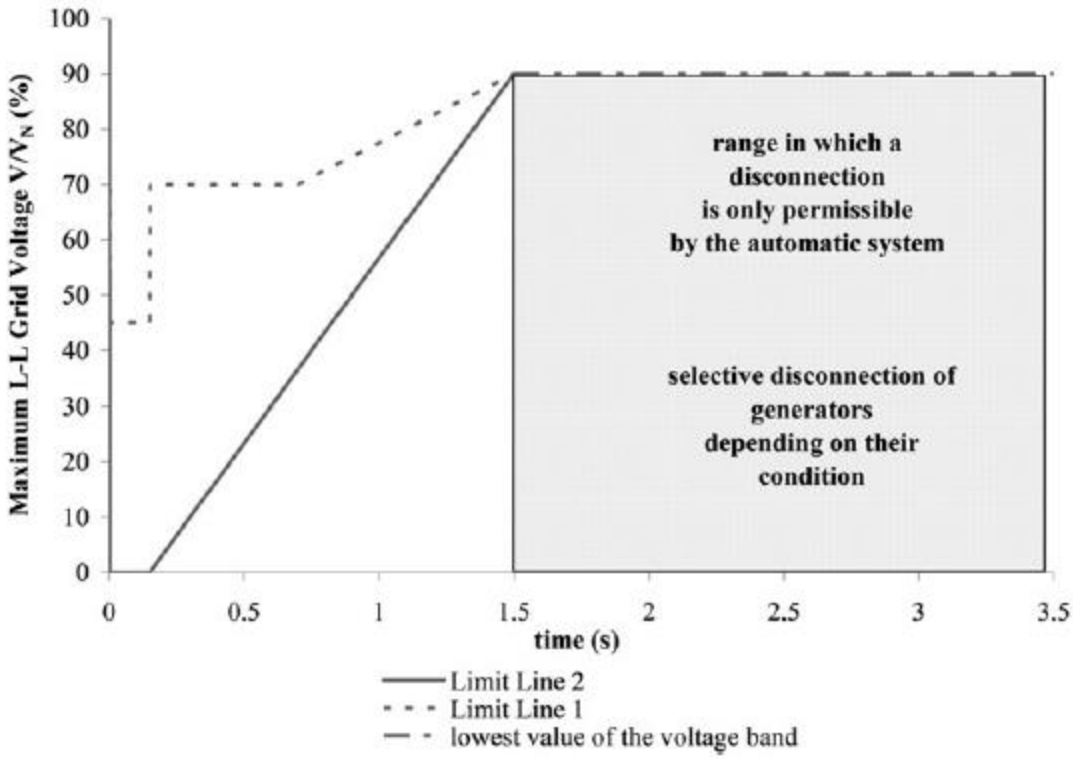

Figure 2-3 : Minimum FRT requirements according to the E.ON grid code [10]

In Germany, as shown in Figure 2-3, wind generators are required to stay connected to the grid for voltages within the limit lines 1 and 2 whereas they should be disconnected from the grid if the voltage at the low voltage side of the generator transformer drops below the limit line 2. According to the minimum FRT requirements of the E.ON grid code depicted in Figure 2-3, wind generators should withstand voltage drops down to 0% of the nominal voltage at the point of common coupling (PCC) for durations up to 150 ms. The maximum voltage dip duration is 1.5 s. After this time, the automatic protection system must disconnect the wind generators depending on the voltage sag at the low voltage side of their respective transformers.

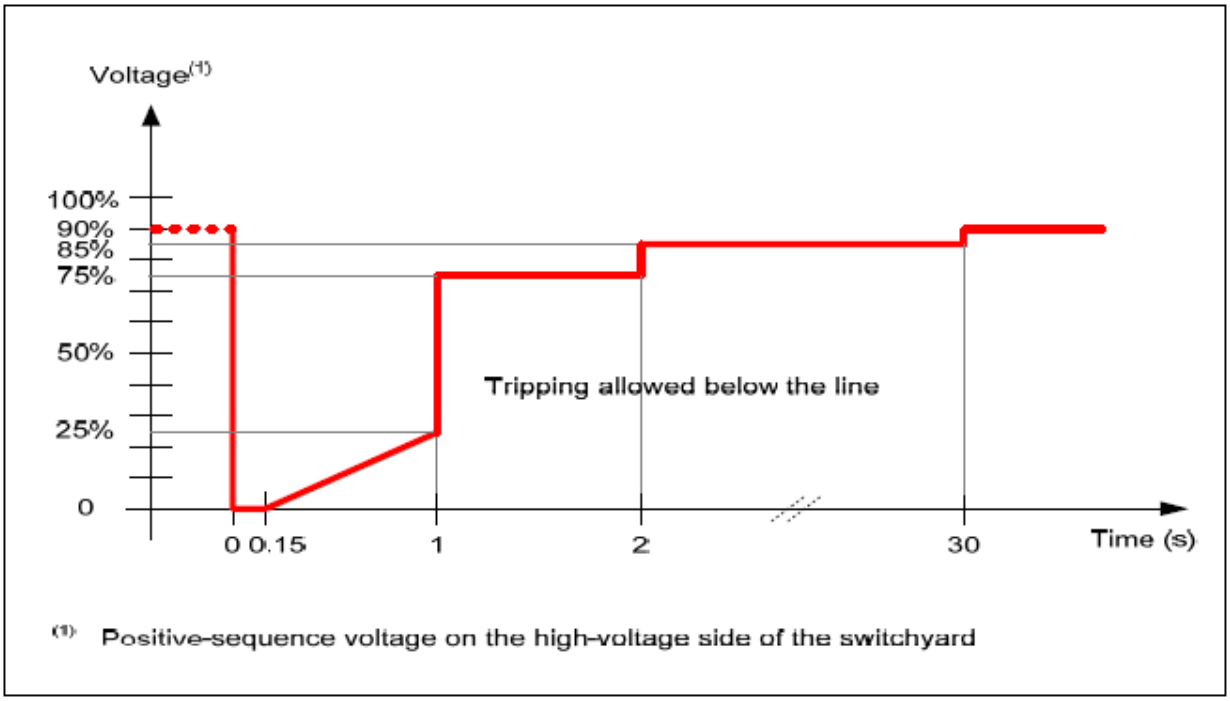

Figure 2-4 : Minimum FRT requirements according to Hydro-Québec grid code [32]

In the province of Quebec, as shown in Figure 2-4, wind generators are required to stay connected to the grid for voltages above the red line whereas disconnection is allowed if the positive sequence voltage at the high voltage side of the switchyard drops below the red line. According to the minimum FRT requirements of the Hydro-Québec grid code, wind generators should withstand voltage drops down to 0% of the nominal voltage for durations up to 150 ms. Wind generators must stay connected to the grid for voltage dips at the high voltage side of the switchyard within 0.75 to 0.85 p.u. which last less than 2 s and voltage dips within 0.85 to 0.9 p.u. which last less than 30 s They must always remain in service for voltage dips greater or equal to 0.9 p.u [32]. For a particular FRT curve, the wind turbine must remain connected to the grid for voltage dips above the limit line whereas the wind turbine should be disconnected from the grid for voltage dips below the limit line. In this respect, grid codes of Germany and the province of Quebec appear to be among the more restrictive grid codes as they require wind farms to withstand voltage dips down to 0%. The duration of the prescribed voltage dip depends on the response time of the protection system. According to the latest E.ON grid code [37], wind power plants must withstand maximum voltage dips down to 0% of the nominal voltage for durations up to 150 ms (7.5 cycles). On the other hand, the wind farms connected to Hydro-Québec transmission system via power converters are required to remain operational throughout the

entire voltage range except for voltage levels greater than 1.25 p.u [36]. The minimum time periods during which the wind farms must remain in operation during voltage dips is specified in Figure 2-4.

The E.ON grid code [37] addresses LVRT requirements for symmetrical voltage dips only whereas Hydro-Quebec specifies FRT requirements for both three-phase and unsymmetrical faults affecting the transmission network. It also provides additional requirements for remote symmetrical and unsymmetrical faults cleared by slow protective devices (up to 45 cycles) [36], [10], [32].

2.4.2 Active power restoration

Most grid codes include provisional requirements to ensure fast restoration of the active and reactive power to the pre-fault levels right after fault clearance [10]. The German grid code requires the pre-fault active power to be completely restored 5 s after fault clearance [10]. As for Hydro-Quebec, no specific requirement has been set up regarding the restoration of active power in-feed [32].

2.4.3 Reactive current injection for voltage support

In networks with significant wind penetration, wind turbine generators are expected to support and fast restore the grid voltage in the same way as conventional generators by injecting additional reactive current into the network during disturbances [10]. In Germany, the required reactive current injection must start one cycle after the fault is detected, for voltage drops or rises larger than 10% of the WT nominal voltage (5% in case of offshore wind farms). The minimum reactive current injection is defined in Figure 2-5.

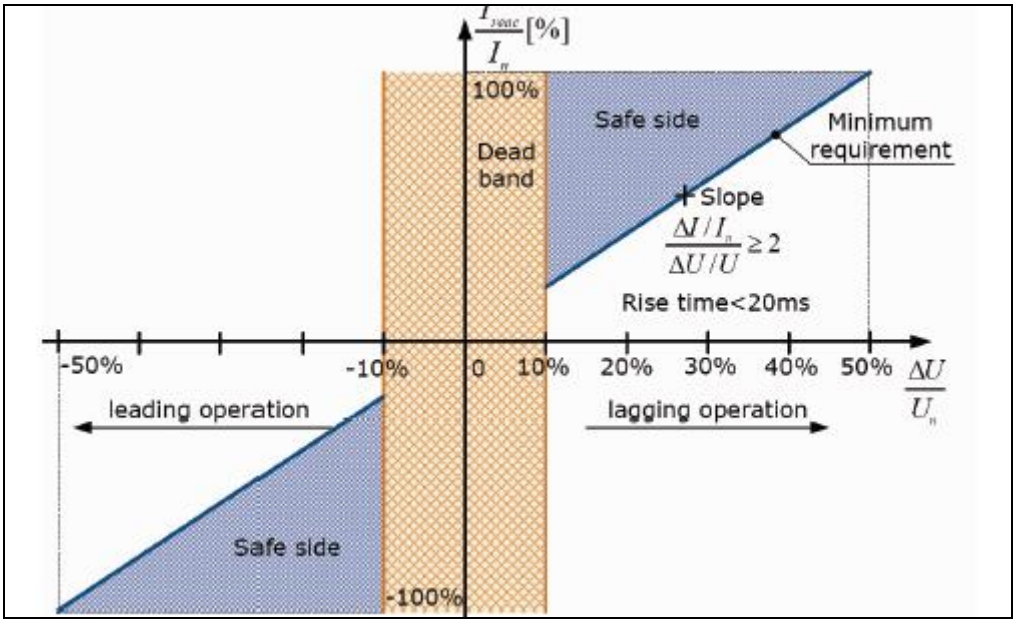

Figure 2-5 : Reactive current injection according to the German grid code [9].

As for wind power plants connected to the transmission network, they are required to operate within minimum leading or lagging rated power factor of 0.95 under normal and abnormal operating conditions [32]. Wind turbines must be able to supply or absorb reactive power over the entire power generation range [36].

For the purpose of steady-state short-circuit analysis, the assessment of fault current contribution of full converter wind turbine generators is only relevant if FRT requirements are adequately accounted for.

CHAPITRE 3 DETAILED STUDY OF TYPE 4 WTG UNDER FAULT CONDITIONS

EMTP-Type programs allow modeling in detail the behavior of a Type 4 WTG while this is not the case yet in current steady-state-type packages [41]. However, steady-state-type packages are still widely used to perform short-circuit analysis for planning purposes rather than using electromagnetic transient programs. Although the latter are based on several assumptions and simplifications which may introduce errors [35], traditional use of power system analysis tools like the symmetrical components [34] explains that, nowadays, traditional short-circuit computation packages are still used more extensively than time-domain programs.

In this chapter, a detailed study of Type 4 WTG under various fault conditions has been performed using EMTP-RV [2]. The detailed model used will help assess the behavior of the Type 4 WTG under grid disturbances to later propose a simplified model which reproduces the real behavior of the WTG under fault conditions.

3.1 Description of the study network

The network studied is simple and is represented in the single-line diagram of Figure 3-1

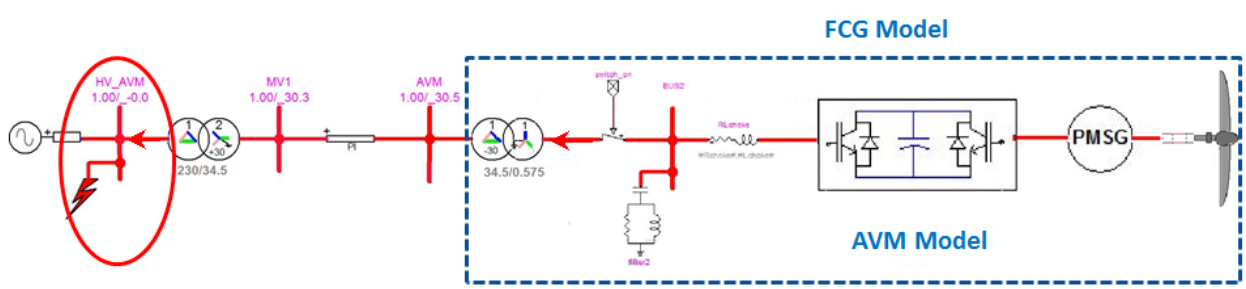

Figure 3-1 : Single-line diagram of the benchmark network

The network consists of 1x2 MW (2.22 MVA) wind turbine generator connected to a 34.5kV Distribution System at the Point of Common Coupling (PCC) through a 2.5 MVA, 0.575/34.5 kV step-up transformer. A collector line, which data is presented in Table 3-1, connects the PCC to the 230 kV grid through a 34.5/230 kV step-up transformer. The grid is represented

by an equivalent source with a short-circuit power of 2500 MVA. The transformers used in this network have respectively YgD and DYg connections. The impedance of both transformers has a value of 6.0%.

As shown in Figure 3-1, the main components of the FCG are the Permanent Magnetic Synchronous Generator (PMSG), the back-to-back VSC and the wind turbine. For the purpose of this validation test, the average mean value model of EMTP is used rather than the detailed model since detailed representation of IGBT switches is not required for steady-state simulations. Figure 3-1 also shows the protection switch which isolates the FCG from the PCC when maximum (or minimum) values are exceeded. Although not shown, the FCG is equipped with a control system which allows independent control of active and reactive power of the wind generator. For this validation test, the reactive power control (i.e. Q control) mode was selected. As a result, a PI controller is used to compare the reference (Qref_pu) with the measured reactive power. Finally, the FCG is equipped with a current limiter which limits the converter current reference in the dq0 frame to a pre-set value of 1.1pu.

Table 3-1 - Transmission line data

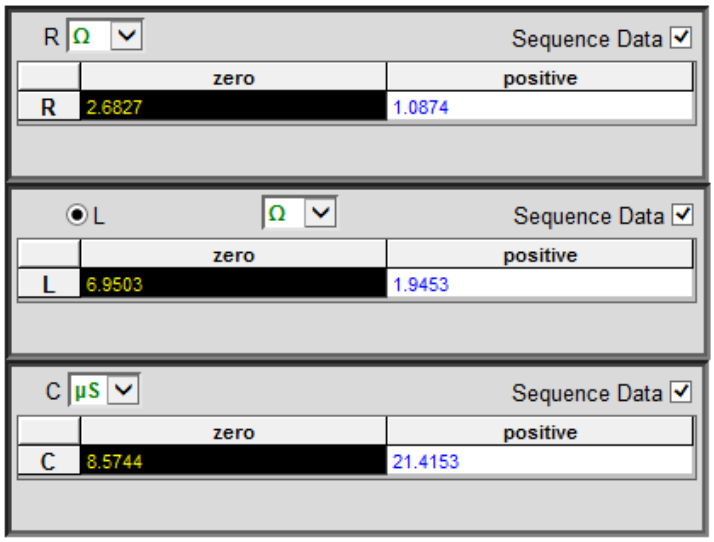

3.2 Fault contribution of Type 4 WTG under various fault conditions

Three phase (LLL) fault and single line-to-ground (LG) fault are respectively applied at the HV-AVM bus which is also considered to be the point of common coupling (PCC) of the wind turbine to the grid. Their effect on the full converter based WTG along with the fault contribution of the WTG are discussed hereafter. In particular, currents injected into the HV-AVM bus are monitored, along with the current injected into the AVM bus, measured at the LV side of the FCG's step-up transformer. This is to have, later on, a good basis of comparison between the current contribution of the detailed model of FCG in EMTP-RV and the contribution of the proposed model. Actually, in EMTP-RV, the wind power plant model includes not only the FCG, but also its step up transformer, the collector line and the step-up transformer which connects the FCG to the grid. Consequently, the fault contribution of the FCG corresponds to the current injected to the grid, into the HV-AVM bus. In CYME 7.0 however, the FCG model doesn't include either the step-up transformers or the collector line. As a result, the fault contribution of the FCG corresponds to the current injected at the LV side of the FCG step-up transformer. Since the objective of this research work is to integrate the proposed model in CYME 7.0, the same approach as currently used in CYME 7.0 is followed and the FCG is modeled such to reproduce its fault contribution at the LV side of its step-up transformer. Other types of equipment pertaining to the wind power plant are modeled separately. Therefore, although one should be interested by the fault contribution of the FCG at the HV-AVM bus, as it is the case in EMTP-RV, later, for validation purposes, the current at the LV side of the FCG's step-up transformer will be considered as the fault contribution of the FCG to the grid. As a result, this current will be analyzed as well in this study.

3.2.1 Three-phase fault (LLL)

A three-phase fault is applied at the PCC at 1.0 s and is cleared after 1.15 s. As illustrated in Figure 3-2, the voltage at the PCC rapidly drops to 0 p.u. as a result of the LLL fault and is restored as soon as the fault is cleared.

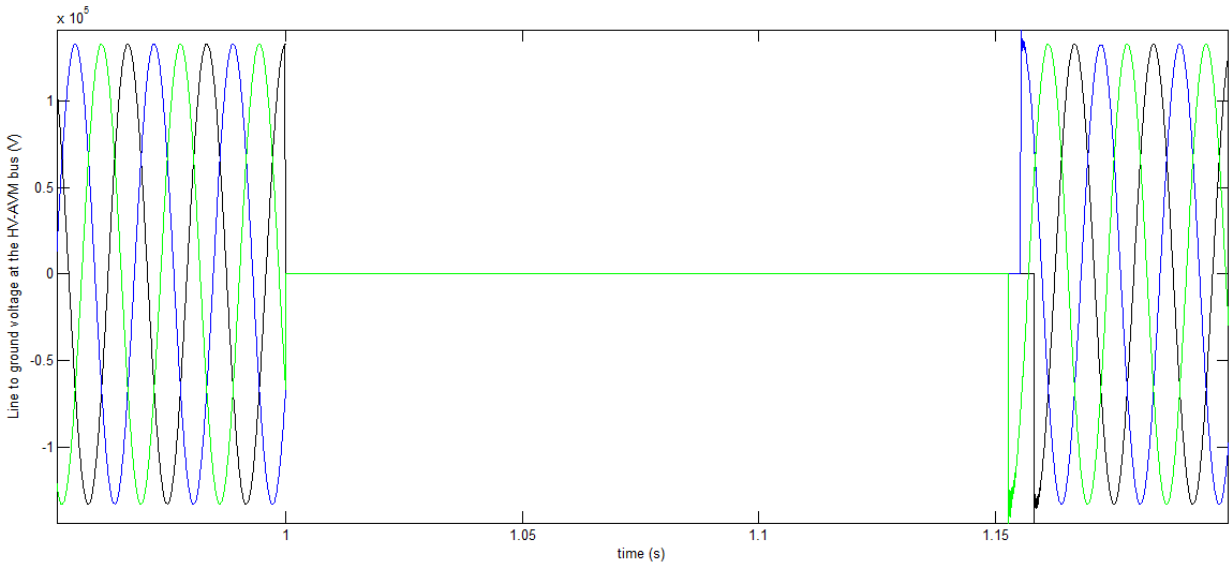

Figure 3-2 : Voltage at HV-AVM bus (PCC) for a LLL fault

Following the reactive power control strategy applied, the FCG remains connected to the grid and provides a fault current contribution of 1.22 p.u. as shown in Figure 3-3.

The FCG fault contribution remains within the limit of the converter's current limiter as, in the dq0 frame, the contribution of the FCG doesn't exceed the maximum pre-set value of 1.1 p.u. as shown in Figure 3-4.

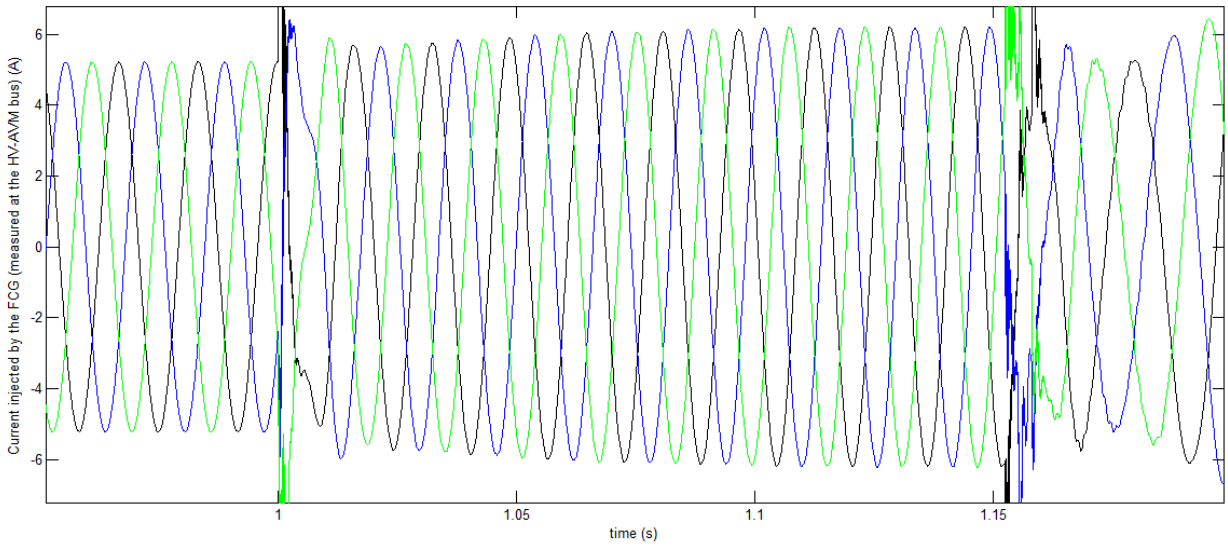

Figure 3-3 : Fault current of the FCG (measured at the HV-AVM bus) for a LLL fault

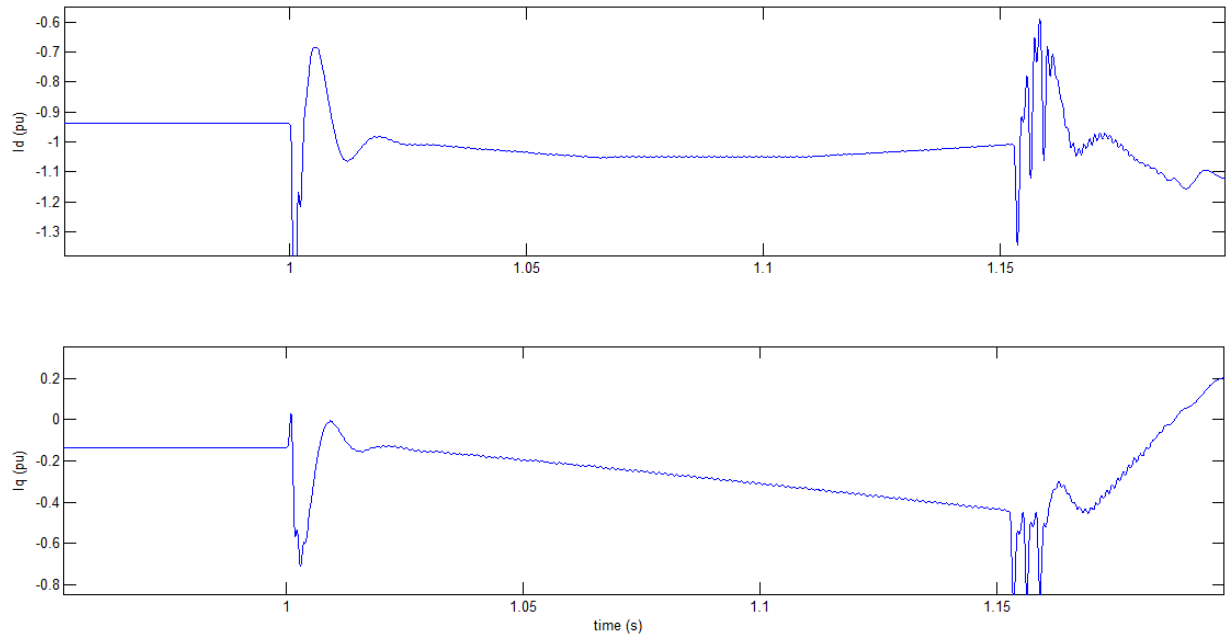

Figure 3-4 : VSC current in the dq0 frame for a LLL fault

To assess whether the current injected into the AVM bus is balanced or not, the sequence currents injected by the WTG into the HV-AVM bus are also monitored as shown in Figure 3-5.

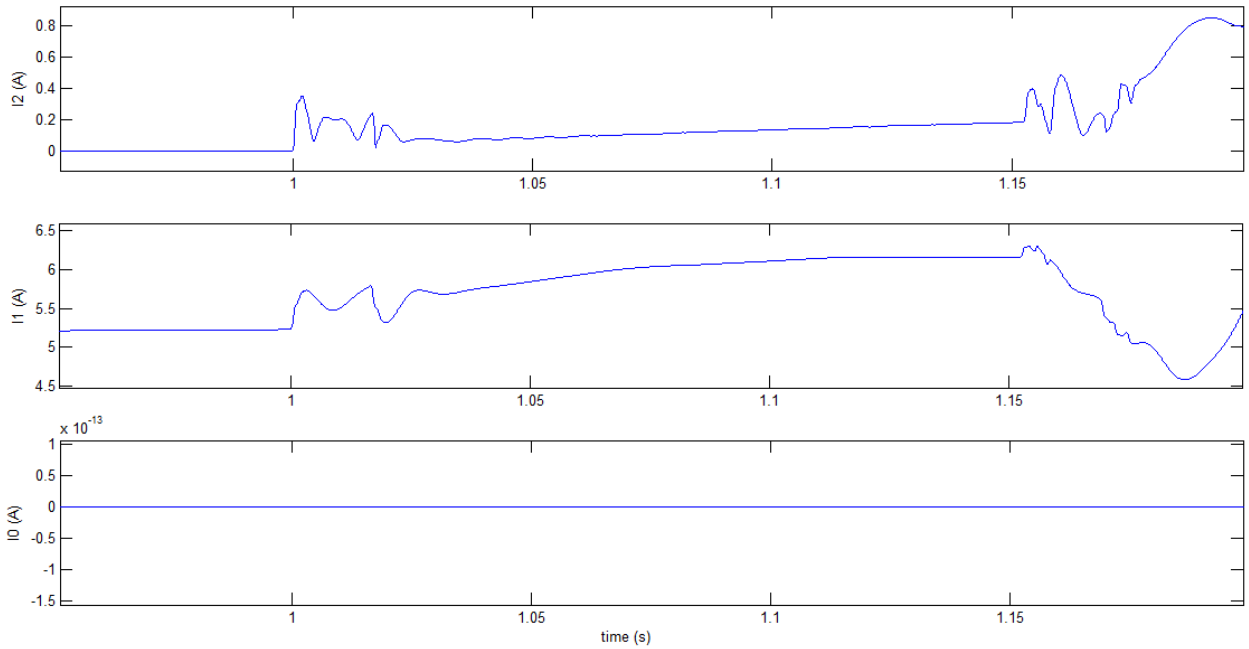

Figure 3-5 : Sequence currents of the FCG (at the HV-AVM bus) for a LLL fault

Figure 3-5 shows that, consecutive to the LLL fault at the HV-AVM bus, although the FCG doesn't provide any zero-sequence current, it does provide a maximum positive sequence current of 6.158 A. It also provides a maximum negative sequence current of 0.178 A which represents 2.9% of the positive-sequence current provided by the FCG.

Consecutive to the LLL fault at the HV-AVM bus, the same observations are made at the LV side of the FCG's step-up transformer. As shown in Figure 3-6, the current contribution of the FCG increases up to 1.22 p.u. as a result of the reactive power control strategy. No zero-sequence current is monitored at the LV side of the FCG's step-up transformer. However, the FCG does inject negative sequence current into the grid as shown in Figure 3-7. The proportion of negative sequence current injected is still very low as it represents only 2.9% of the sequence current injected.

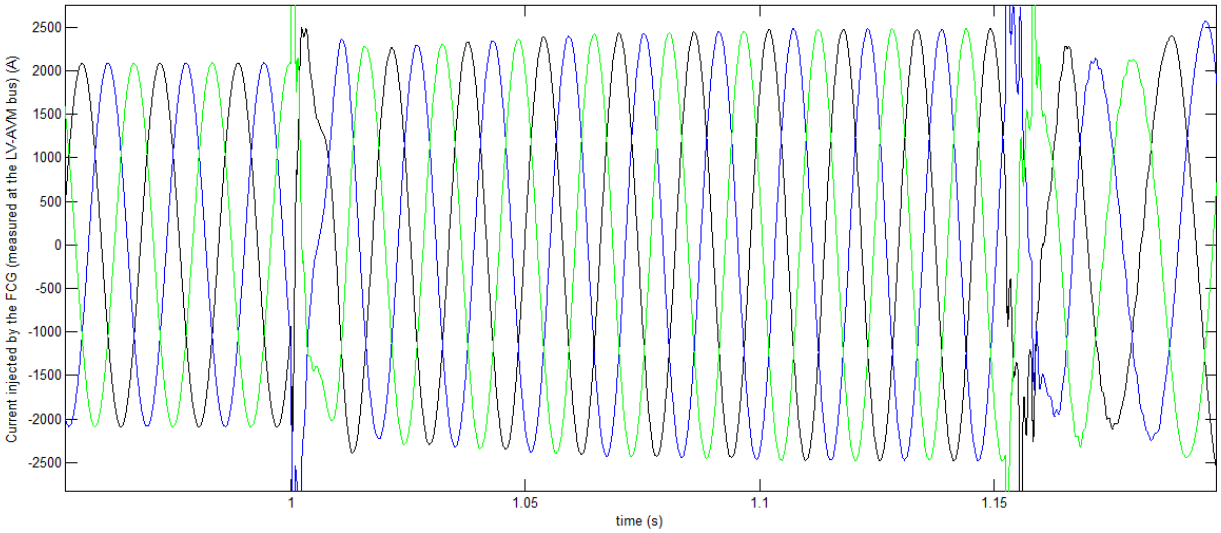

Figure 3-6 : Fault current of the FCG (at the LV side of its transformer) for a LLL fault

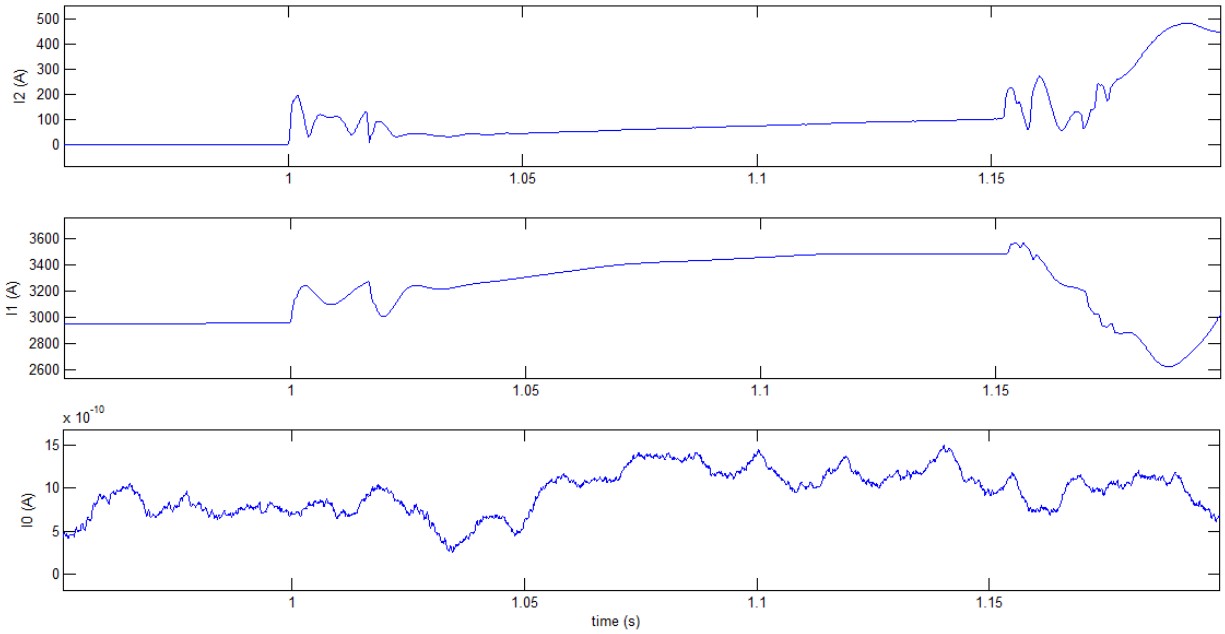

Figure 3-7 : Sequence currents of the FCG (at the LV side of its transformer) for a LLL fault

3.2.2 Single line-to-ground fault (LG)

A single line-to-ground fault is applied at the PCC at 1.0 s and is cleared after 1.15 s. As illustrated in Figure 3-8, the voltage on the faulted phase A rapidly drops to 0 p.u. as a result of the LG fault and is restored as soon as the fault is cleared.

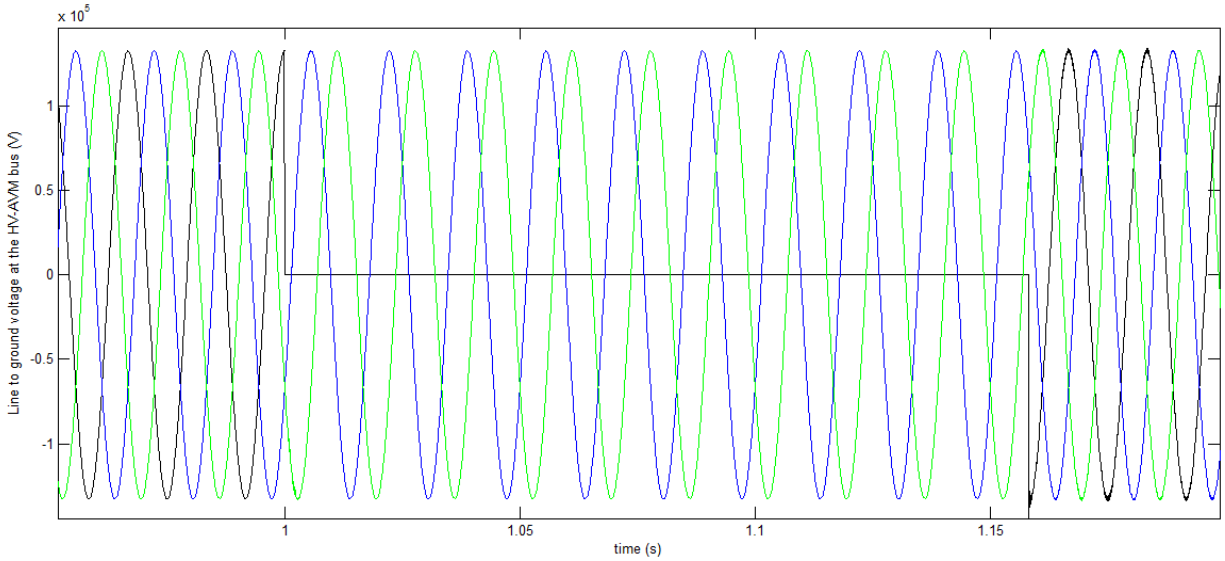

Figure 3-8 : Voltage at HV-AVM bus (PCC) for a LG fault

Following the reactive power control strategy applied, the FCG remains connected to the grid and provides a fault current contribution of 1.23 p.u. as shown in Figure 3-9.

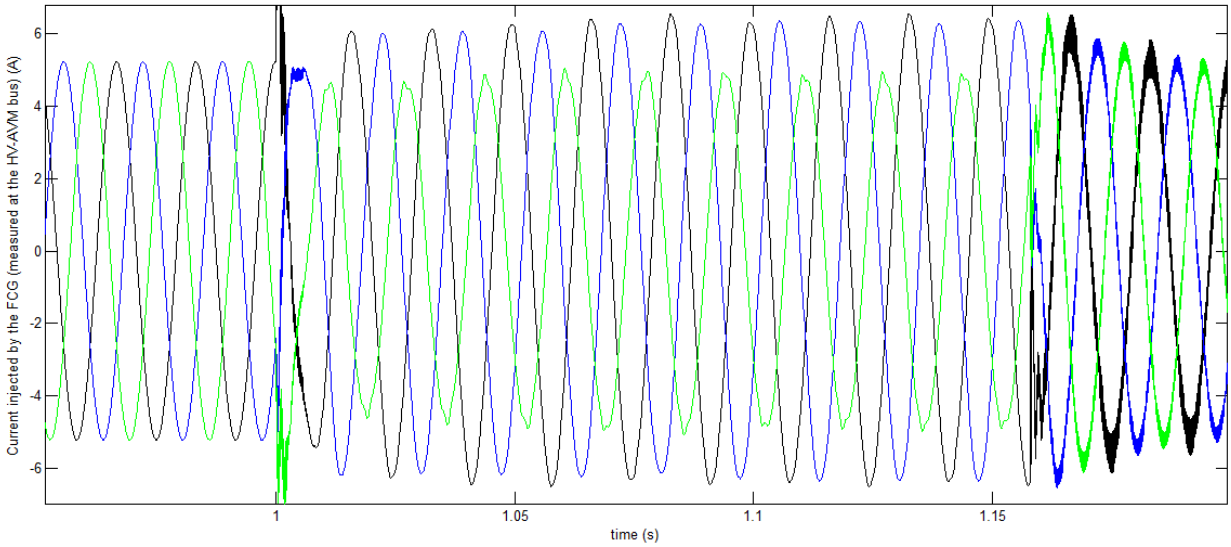

Figure 3-9: Fault current of the FCG (measured at the HV-AVM bus) for a LG fault

Like for the LLL fault, the FCG fault contribution remains within the limit of the converter's current limiter as, in the dq0 frame, the contribution of the FCG doesn't exceed the maximum pre-set value of 1.1 p.u. as shown in Figure 3-10.

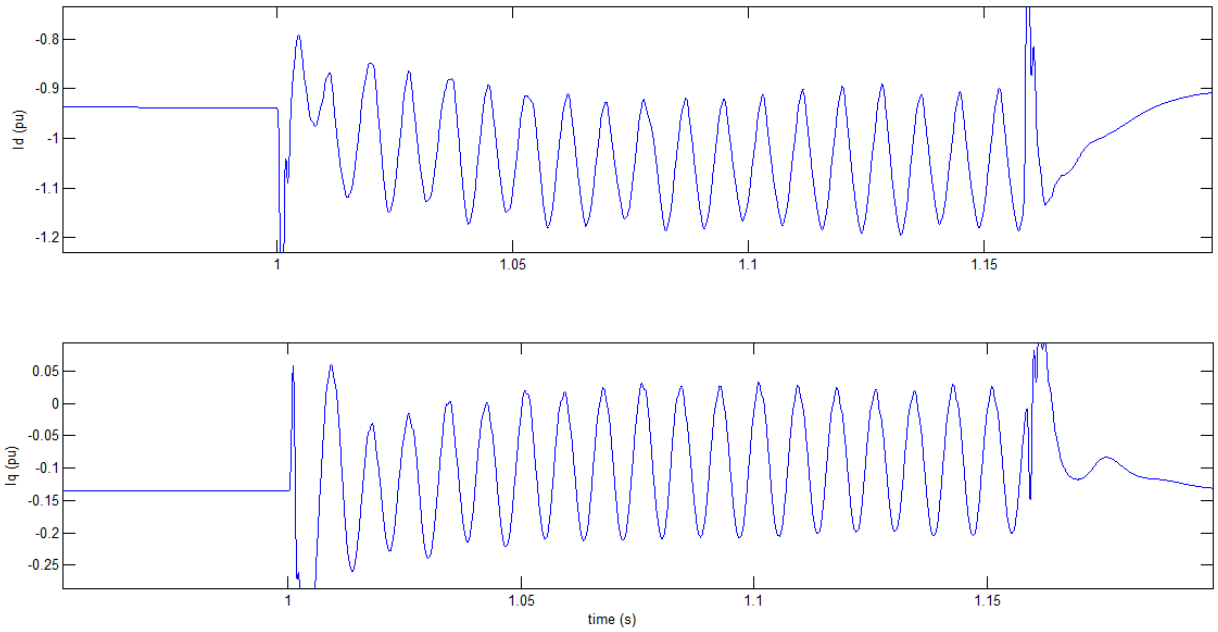

Figure 3-10 : VSC current in the dq0 frame for a LG fault

Figure 3-11shows that, consecutive to the LG fault at the HV-AVM bus, although the FCG doesn't provide any zero-sequence current, it does provide a maximum positive sequence current of 5.861 A. It also provides a maximum negative sequence current of 0.929 A which represents 15.9% of the positive-sequence current provided by the FCG.

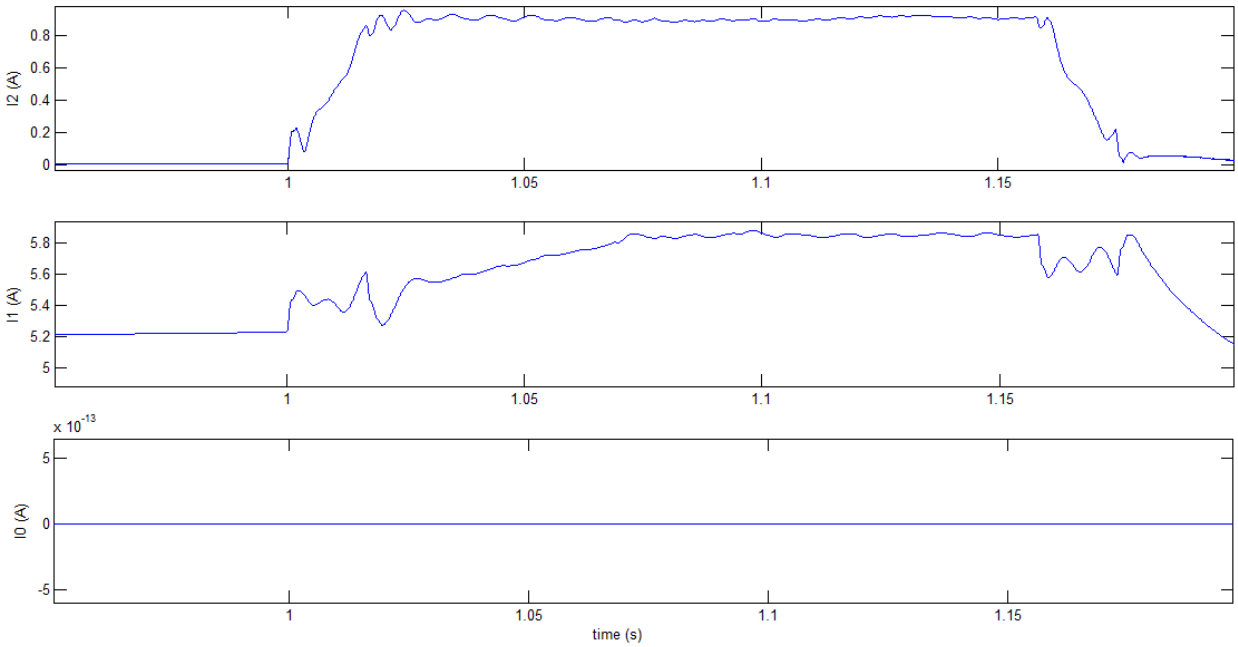

Figure 3-11 : Sequence currents of the FCG (measured at the HV-AVM bus) for a LG fault

Consecutive to the LG fault at the HV-AVM bus, the same observations are made at the LV side of the FCG's step-up transformer. As shown in Figure 3-12, the current contribution of the FCG increases up to 1.23 p.u. as a result of the reactive power control strategy. No zero-sequence current is monitored at the LV side of the FCG's step-up transformer. However, the FCG does inject negative sequence current into the grid as shown in Figure 3-13. For the LG fault, the proportion of negative sequence current injected is quite significant as it represents 15.5% of the sequence current injected.

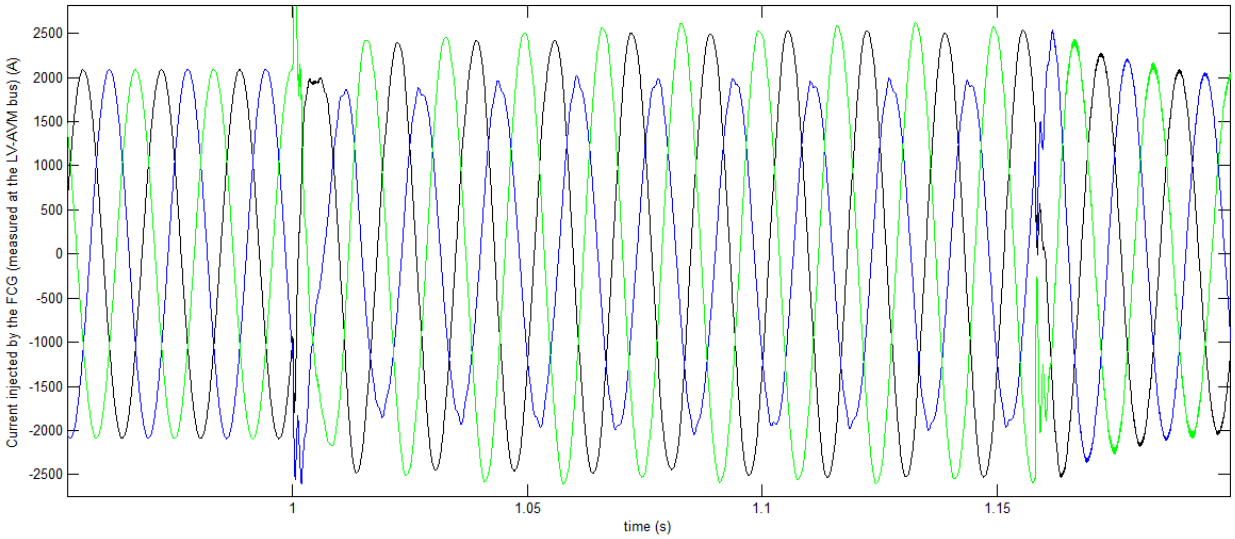

Figure 3-12 : Fault current of the FCG (at the LV side of its transformer) for a LG fault

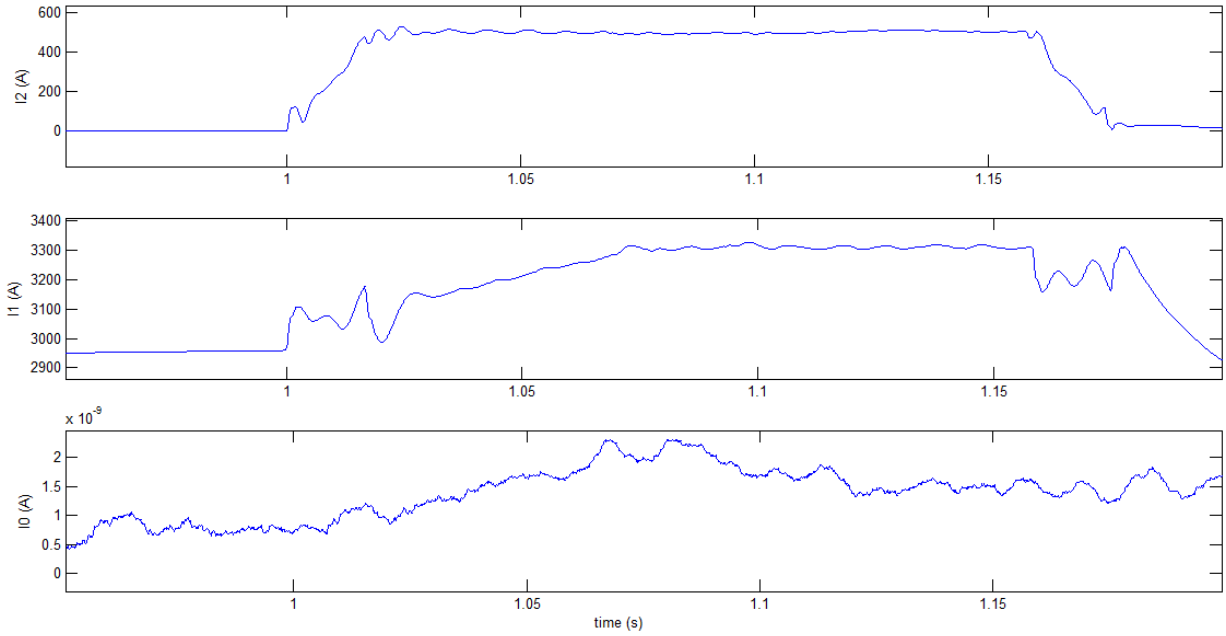

Figure 3-13 : Sequence currents of the FCG (at the LV side of its transformer) for a LG fault

CHAPITRE 4 SHORT-CIRCUIT ANALYSIS IN NETWORKS WITH TYPE 4 WTG

4.1 Purpose of short-circuit studies

Short-circuit studies consist in determining the maximum and minimum short-circuit currents in an electrical network. They are typically performed at the planning level to adequately select and dimension the various types of electrical equipment on the network. They are also used by power system operators for the design and selection of interrupting equipment and for the proper setting and coordination of the system protective devices. Fault currents generally depend on the network topology, the type of fault and its location and the number and type of generators in service [19].

The connection of DG sources is regulated by interconnection requirements on voltage regulation, power quality constraints and operation under abnormal conditions. Regarding the latter, it is required that the total fault level, determined by the combined short-circuit contribution of the upstream grid and the DG, is lower than the network design value [1]. At the distribution level, networks often operate close to their design short-circuit capacity. This can be an inhibiting factor for the interconnection of DG sources to the network [1]. Therefore, when adding power generating capabilities to an existing system, short-circuit studies are particularly important to assess their impact on the grid's fault current levels. The fault contribution of wind energy conversion systems (WECs) has long been ignored since wind turbines were supposed to be disconnected after a fault. This was known as islanding. However, with the increased penetration level of wind power, utilities are forced to revise their grid code requirements and wind turbines are now expected to support the grid voltage during a fault. For this reason, their contribution to the fault level of the network can no longer be ignored.

In order to keep guarantying the safe and economical operation of electrical networks, power analysis programs should closely reproduce the real behavior of wind turbines, especially during abnormal operating conditions. Electromagnetic Transient type programs like EMTP-RV do provide accurate models of WECs to estimate their contribution under abnormal conditions but

traditional short-circuit computation packages are still more widely used to perform short-circuit studies of electrical networks.

Standard calculation methods like IEC 60909 [3] have been developed to calculate the fault contribution of various grid elements. However, they are not applicable to full scale converter based WTG as their fault contribution don't depend on the electrical characteristic of the generator. The latter is indeed completely decoupled from the grid. Hence, the fault contribution of full converter based DG sources rather depends on the type of interface with the grid, the voltage before the fault, the operating mode, the technology used, etc.

4.2 Literature review

With the increased penetration level of wind power plants interfaced with the grid via full scale frequency converters and the progression of FRT requirements in several countries, recent studies have shown that the fault current contribution of WTG cannot be disregarded anymore. In some cases for instance, plants contribution to the short-circuit level at the substation HV bus after the installation of DG units has appeared to be as high as six or more times the rated turbine current [13].

For this reason, valuable effort has already been provided in modeling the behavior of inverter interfaced wind power plants and their effect on the design short-circuit level of distribution networks. However, when addressing the modeling of Type 4 WTG, many frequency domain short-circuit packages don't model adequately the effect of the full scale frequency converter on the fault contribution of the WTG [41]. Besides, traditional short-circuit analysis methods are barely adapted to determine the fault current contribution of Type 4 WTG ([3], [4], [12]).

Actually, no standard addresses the modeling of full scale converter based WTG. The standard on DG interconnection [11] simply states that the fault current of ECG usually ranges within 1.2 to 1.5 p.u. without further explanations. As for [3] it doesn't provide any guideline on the modeling of Type 4 WTG.

In short-circuit analysis, sources are conventionally represented by an ideal voltage source behind an impedance. This is the case for synchronous generators, induction generators and motors. As a result, an approach presented in [12] proposes using the E/Z simplified method to represent the

detailed model of the wind power plant as a 1 p.u. voltage source followed by an equivalent series impedance. These impedances can be used later on in short-circuit calculations for relay settings in the transmission network [13].

In [1], the IEC Standard 60909 is extended to assess the impact of DG sources on the fault level of medium and low voltage distribution networks. Based on experience and available information on Type 4 WTG, it is proposed to adopt a constant current representation estimated at 2 p.u. Besides, due to the impossibility of adequately determining the phase angle of the current contribution, it is proposed to algebraically add the fault contribution of the Type 4 WTG to the total fault level of all other sources.

In [15] and [16], only the maximum fault contribution of full scale converter interfaced WTG is discussed and is typically considered ranging between 1.0 to 4 p.u. of its rated current depending on the overcurrent capability of its power converter. The upper values such provided generally correspond to a three-phase fault at the WT terminals and the fault contribution of the Type 4 WTG is expected to decrease with distance from the WTG [16].

In [17], although stated upfront that the fault contribution of the Type 4 WTG mainly relies on the power converter's control algorithms, the behavior of the Type 4 WTG under steady-state fault conditions is later simply described from a theoretical standpoint. The fault contribution of the WTG is said to be limited at or 10 % above its rated current for three-phase fault without further explanations. The fault contribution of the Type 4 WTG is also assumed to be balanced regardless of the type of fault.

In [18] too, the fault contribution of the Type 4 WTG is considered limited at 2 p.u. The proposed method distinguishes two periods during which the behavior of the Type 4 WTG varies. The sub-transient period refers to the first cycle of the fault and corresponds to the peak contribution of the WTG. The transient period follows for 5 to 10 cycles and sees the decrease of the fault contribution of the WTG due to the action of the controller. The sub-transient peak current is estimated based on a Thevenin equivalent which assumes the internal voltage of the WTG constant and set to its pre-fault value. As for the impedance used, it corresponds to the series combination of the grid-side converter filter reactance along with the transformer reactance. In the transient period, the WTG is considered feeding the fault only if its fault contribution has not exceeded its peak current limit during the sub-transient period. In that case, the fault contribution

of the Type 4 WTG is updated dynamically according to the feeder fault response by adjusting the internal voltage of the WTG equivalent model.

A model specific to ENERCON WECs but applicable to any full scale converter based WTG is presented in [19]. To fit the standard steady-state short-circuit calculation methods, the WTG is modeled as a voltage source behind impedance rather than a controlled current source. The equivalent model is developed in sequence domain and is based on the worst case scenario, considered to be the injection of the WTG maximum current at a phase angle of 90 degree. The equivalent positive sequence impedance of the WTG is determined accordingly and considered as purely reactive. As for the negative and zero sequence impedances, they are considered as infinite to reproduce a balanced fault current injection. The value of the internal voltage of the WTG is constant and set at the value of the low voltage terminal of the WTG after occurrence of the fault. Besides, unlike in [9], the value of the maximum fault contribution is specific to the WTG.

In [20], it is stated that, for the purpose of steady-state short-circuit analysis, the fault contribution of full scale converter based WTG is assumed similar in sub-transient, transient and steady-state fault conditions. Instead, the fault contribution of electronically coupled WTG is said to depend on the distance to fault from the WTG. As a result, it is proposed to adopt two distinct models to assess the fault contribution of the WTG: a current source set to the maximum fault contribution for close faults and a constant PQ source for remote faults. Problem in implementing such a model remains as it is hard to differentiate a remote from a near fault.

In [21], an extended Gauss-Seidel load-flow based approach is proposed to assess the fault contribution of grid-connected inverter dominated networks. The inverter-based WTG are modeled as current constrained PQ nodes behind a coupling reactance during the sub-transient and transient periods. Additionally, when the low pass filter on the grid-side fails to sufficiently attenuate the negative sequence component caused by unbalanced fault conditions, the WTG is modeled as a constant positive sequence current source in parallel with the filter capacitor. As soon as the fault contribution of an inverter exceeds the converter's threshold, its model is switched to a current source set to a pre-defined value, typically 2 p.u.

The modeling of Siemens Type 4 WTG is specifically addressed in [22]. The WTG is considered providing balanced currents even for unbalanced types of faults. The article discusses only the maximum contribution of the Siemens Type 4 WTG and also distinguishes two time periods for

which the fault contribution of the WTG differs. In the first period lasting half a cycle, the current contribution of the WTG is limited to 2.5 p.u. whereas in the second period, the current injected to the grid is limited to a required FRT value, namely 2% lagging reactive current increase for every 1% drop in positive sequence voltage 90% of nominal voltage. This results in a typical fault contribution between 1.1 to 1.2 pu.

In [23], the contribution of Type 4 WTG is assumed not to exceed 1.5 p.u. Besides, it is assessed that the impact of Type 4 WTG depends not only on the size of the machine but also on its location as, when located at the end of the line, they barely affect the feeder breaker fault duty.

Another interesting contribution from [9] proposes modeling wind turbines with full rating power converters as a Thevenin equivalent which is iteratively adjusted by a general routine to fit the model with the expected FRT behavior specified in the German grid code. The interest of this method is that the proposed model of Type 4 WTG doesn’t require using proprietary data from specific WT manufacturers. However, the method appears to be tedious to implement and its convergence is not guaranteed for all network topologies.

When it comes to variable speed wind turbine generators, the Joint Working Group on Wind Plant Short Circuit Contribution co-chaired by R. Walling [25] not only estimates that the complex behavior of Type 4 wind turbine generators cannot be represented by a simple Thevenin equivalent but also recommends adapting short-circuit algorithms to accurately represent the short-circuit current contribution of wind turbine generators. In [24] and [25], the short-circuit behavior of Type 4 WTG is compared to a limited current source which magnitude depends on the time period that is considered. Indeed, to better evaluate the behavior of Type 4 WTG under fault conditions, it is recommended to consider two distinct time periods between which the behavior of the Type 4 WTG changes. In the first one to two cycles after occurrence of the fault, the fault contribution of the WTG mainly depends on the pre-fault operating conditions and the fault contribution of the WTG ranges between a minimum value corresponding to the pre-fault load current to a maximum fault contribution that can go up to 2 to 3 p.u. After detection of the fault, the fault contribution of the WTG mainly depends either on the applicable FRT requirements or on the control strategy implemented by the WT manufacturers. In such case, the fault contribution of the WTG can range between zero amps to a maximum of 1.5 p.u.; depending on the overcurrent design capability of the converter. The article only provides recommendations

but doesn't provide any model for the representation of Type 4 WTG for short-circuit analysis. It is however mentioned that in case current sources cannot be modeled directly in the short-circuit analysis method chosen, an equivalent voltage behind impedance model must be adopted and adjusted iteratively to match the desired fault contribution. This is hardly applicable unless the WTG is assumed to always contribute up to its maximum value regardless of the type of fault and location.

As for the models currently implemented in commercial short-circuit analysis software tools [41], they don't appropriately handle either the short-circuit contribution of Type 4 WTG. In the general multiphase network representation adopted by CYME to perform short-circuit analysis, electronically coupled generators are treated the same way as induction generators, that is, a voltage source followed by a sub-transient impedance Z''. Like for induction generators, the equivalent voltage source representing the ECG is considered ungrounded, i.e. with infinite zero-sequence impedance. Hence, ECGs are modeled as delta connected induction generators. As for Z'', it is derived from the maximum three-phase fault contribution of the inverter, which corresponds to a percentage of the rated current of the WTG. The detailed model of ECG as implemented in CYME 7.0 is shown below:

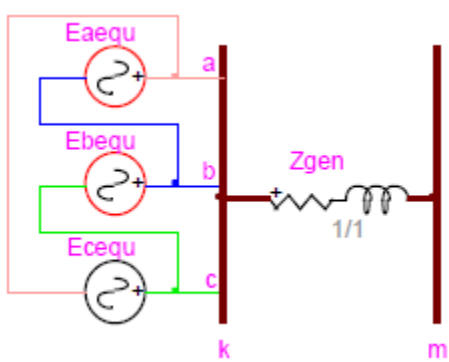

Figure 4-1 : Full converter based WTG model in CYME 7.0

The value of E_{equ} depends on the pre-fault voltage. If short-circuit calculations start at nominal value:

$$E_{equ} = V_{NOM} \tag{2.3}$$

where:

V_{NOM} : Line-to-neutral rated voltage of the WTG.

If short-circuit calculations start at load flow solution:

$$E_{equ} = V_{LF} + Z1_{wecs}.I_{LF} \tag{2.4}$$

where:

V_{LF} : Magnitude of line-to-neutral pre-fault voltage of the WTG (p.u.).

I_{LF} : Pre-fault line current of the WTG (p.u.).

$Z1_{wecs}$: Sub-transient impedance of the WTG (p.u.).

On the other hand, in CYME 7.0, regardless of the pre-fault conditions assumed, the sub-transient impedance Z'' is always calculated as:

$$Z'' = Z1_{wecs} = -j\frac{1}{I_{wecs_\max}} \tag{2.5}$$

where:

$I_{wecs_\max}$: Maximum three-phase fault contribution of the full converter WTG (expressed in p.u. based on the converter rated current).

The impedance Z'' represents the direct sequence impedance as a full converter WTG only injects direct sequence current into the grid. The negative and zero sequence impedances of the WTG are both considered as infinite.

It is obvious from equation (2.5) that when short circuit starts at load flow solution, the impedance of the WTG is not calculated correctly since it assumes that the equivalent source is at 1 pu instead of its real value. Hence, according to equation (2.4), E_{equ} is not calculated correctly either.

CHAPITRE 5 SHORT-CIRCUIT MANA MODEL FOR TYPE 4 WTG

The fault contribution of Type 4 WTG strongly relies on the control strategy applied before the fault and on the FRT capabilities either set by applicable grid codes or implemented by a specific manufacturer.

In [26], two time periods are distinguished to adequately estimate the contribution of a Type 4 WTG under fault operating conditions: during fault detection (1 to 2 grid cycles) and after fault detection.

During the first two cycles following the occurrence of a fault, the WTG tends to behave according to its operating control mode. It provides only direct sequence currents under both balanced and unbalanced conditions; except in some specific cases [27]. However, its fault contribution is limited by the overload capacity of the converter which is typically 110 to 150% of the rated current. Therefore, when the converter is saturated, the WTG behaves as a current source providing the maximum fault contribution.

After fault detection, the fault contribution of the Type 4 WTG is determined either by the applicable grid codes or by the inverter control strategy implemented by a specific manufacturer. Several grid codes require the WTG to stay connected to the grid under abnormal conditions and also to provide voltage support by injecting a pre-specified amount of reactive current. Hence, after fault detection, the Type 4 WTG behaves like a voltage controlled current source, injecting only balanced current under any operating conditions.

Based on the observed behavior of the Type 4 WTG under steady-state fault conditions, two models are proposed in this dissertation to assess its fault current contribution in phase domain. The two models reproduce the behavior of the WTG respectively under sub-transient and transient abnormal operating conditions. They are afterwards implemented in an iterative short-circuit algorithm using the MANA approach. As previously stated, these models depend not only on the control strategy applied prior to the fault but also on the FRT capabilities of the WTG.

The multiphase MANA formulation presented in [28] is adopted to represent adequately the constraint equations of the WTG. Besides, due to the iterative nature of the proposed short-circuit

model, a fault flow algorithm based on Newton's method is adopted to perform short-circuit calculations on networks with inverter connected WTG.

5.1 Newton MANA method

Based on the expansion in Taylor series of a matrix function **f(x)** around a given solution $\mathbf{x}^j$, the Newton method allows solving non-linear matrix equations like **f(x) = 0** by reformulating them as:

$$J^j.\Delta x^j = -f^j \tag{2.6}$$

where:

J^j : Jacobian matrix at iteration j.

f^j : Mismatch vector at iteration j.

Δx^j : Computed error at iteration j.

Δx^j is used to update the solution vector **x** such that:

$$x^{j+1}. = x^j + \Delta x^j \tag{2.7}$$

In [28], a Newton-based solution approach is adopted to accommodate controlled devices. In this method, controlled devices are modeled according to their constraint equations. The method consists in using the MANA approach to build an augmented Jacobian matrix which is iteratively updated until matching the constraints set for each controlled device.

The resulting generic matrix equation at given iteration *j* is given by:

$$\begin{bmatrix} \mathbf{Y_n} & \mathbf{A_c} & \mathbf{A_{IL}} & \mathbf{A_{IG}} & \mathbf{0} \\ \mathbf{A_r} & \mathbf{A_d} & \mathbf{0} & \mathbf{0} & \mathbf{0} \\ \mathbf{J_L} & \mathbf{0} & \mathbf{J_{LI}} & \mathbf{0} & \mathbf{0} \\ \mathbf{Y_G} & \mathbf{0} & \mathbf{0} & \mathbf{B_{GI}} & \mathbf{B_{GE}} \\ \mathbf{J_{GPQ}} & \mathbf{0} & \mathbf{0} & \mathbf{J_{GPQI}} & \mathbf{0} \\ \mathbf{J_{GPV}} & \mathbf{0} & \mathbf{0} & \mathbf{0} & \mathbf{0} \\ \mathbf{J_{GSL}} & \mathbf{0} & \mathbf{0} & \mathbf{0} & \mathbf{0} \end{bmatrix}^j \begin{bmatrix} \mathbf{\Delta V_n} \\ \mathbf{\Delta I_x} \\ \mathbf{\Delta I_L} \\ \mathbf{\Delta I_G} \\ \mathbf{\Delta E_G} \end{bmatrix}^j = - \begin{bmatrix} \mathbf{f_n} \\ \mathbf{f_x} \\ \mathbf{f_L} \\ \mathbf{f_{GI}} \\ \mathbf{f_{GPQ}} \\ \mathbf{f_{GPV}} \\ \mathbf{f_{GSL}} \end{bmatrix}^j \tag{2.8}$$

where:

$\mathbf{Y_n}$: Classical nodal admittance matrix.

$\mathbf{A_r}$: Voltage coefficient matrix for non-linear devices without controls.

$\mathbf{A_c}$: Current coefficient matrix for non-linear devices without controls.

$\mathbf{A_d}$: Adjacency matrix of infinite impedance type devices

$\mathbf{J_L}$: Voltage coefficient matrix for PQ loads.

$\mathbf{J_{LI}}$: Current coefficient matrix for PQ loads.

$\mathbf{Y_G}$: Internal admittance matrix of generators.

$\mathbf{B_{GI}}$: Current coefficient matrix for generators.

$\mathbf{B_{GE}}$: Internal voltages coefficient matrix for generators.

$\mathbf{J_{GPQ}}$: Voltage coefficient matrix for PQ controlled generators.

$\mathbf{J_{GPQI}}$: Current coefficient matrix for PQ controlled generators.

$\mathbf{J_{GPV}}$: Voltage coefficient matrix for PV controlled generators.

$\mathbf{J_{GSL}}$: Voltage coefficient matrix for slack-type buses.

In their detailed form, sub-matrices $\boldsymbol{A_c}$, $\boldsymbol{A_r}$ and $\boldsymbol{A_d}$ presented in equation (2.8) published in [28] and [44] are respectively written as presented below:

$$\boldsymbol{A_c} = \begin{bmatrix} \boldsymbol{V_c} & \boldsymbol{D_c} & \boldsymbol{S_c} \end{bmatrix} \tag{2.9}$$

$$\boldsymbol{A_r} = \begin{bmatrix} \boldsymbol{V_c} & \boldsymbol{D_c} & \boldsymbol{S_c} \end{bmatrix}^T = \boldsymbol{A_c^T} \tag{2.10}$$

$$\boldsymbol{A_d} = \begin{bmatrix} \boldsymbol{S_d} \end{bmatrix} \tag{2.11}$$

where:

$\boldsymbol{V_c}$: Voltage sources adjacency matrix.

$\boldsymbol{D_c}$: Dependency functions matrix.

$\boldsymbol{S_c}$: Adjacency matrix of zero impedance type devices.

$\boldsymbol{S_d}$: Adjacency matrix of infinite impedance type devices

In equation (2.8), f^j is the mismatch vector presented in its detailed form. It represents the mismatch between the desired value of the variable under constraint and its value at iteration *j*.

As for the computed error at iteration *j*, Δx^j, presented in its detailed form in equation (2.8), it corresponds to the error affecting the unknown variables computed between two consecutive iterations. These variables are:

$\mathbf{V_n}$: Nodes voltages.

$\mathbf{I_x}$: Vector containing sources currents, transformers secondary currents and switch currents.

$\mathbf{I_L}$: PQ-loads currents.

$\mathbf{I_G}$: Generators currents.

$\mathbf{E_G}$: Generators internal voltages.

In the Newton formulation presented in equation (2.8), complex elements of each sub matrix are separated into real and imaginary parts such that the matrix equation (2.8) is only filled with real numbers.

The MANA approach used in [28] to build the Jacobian matrix allows adopting a systematic and yet efficient method to integrate into the Jacobian such arbitrary equations like constraint equations as it allows partitioning the latter into matrices which contain all the devices without controls and the remaining block matrices which represent the controlled devices. Devices without controls are modeled as in the classical MANA formulation throughout sub-matrices $\mathbf{Y_n}$, $\boldsymbol{A_c}$, $\boldsymbol{A_r}$ and $\boldsymbol{A_d}$. As for controlled devices, they are represented in the Jacobian according to their control type.

As shown in equation(2.8), the constraint equations for a given controlled device *p* are integrated in the Jacobian through voltage and current coefficient sub-matrices, which can be generally labeled as $\mathbf{J_p}$ and $\mathbf{J_{pI}}$. Subscript **p** can be replaced by subscripts **L** or **G**, respectively for load and generator. Using the Newton's method, these block matrices, along with the corresponding mismatch vector $\mathbf{f_p}$, are updated at each iteration *j* until the constraint equation defined in (2.12) is minimized.

$$\mathbf{J_p^j.\Delta V^j + J_{pI}^j.\Delta I^j = -f_p^{\ j}} \tag{2.12}$$

Load currents ($\mathbf{I_L}$) and generator currents ($\mathbf{I_G}$) are derived respectively from the computed errors $\mathbf{\Delta I_L}$ and $\mathbf{\Delta I_G}$. They are included in the Kirchhoff Law's equations of the Jacobian, through the sub-matrices $\mathbf{A_{IL}}$ and $\mathbf{A_{IG}}$.

5.2 Sub-transient model

Under normal operating conditions, the full scale converter of a Type 4 WTG is generally controlled either to deliver constant output power (PQ) or to achieve voltage regulation (PV) within the converter's design limits. When a fault occurs, the Type 4 WTG tries to maintain the constraints imposed by the control strategy set prior to the fault. Hence, under low voltage conditions, the current contribution of the WTG can increase up to the maximum current limit of the power converter. As a result, during the first two cycles after occurrence of a fault, before the fault is detected, the Type 4 WTG is modeled as a current limited generator, controlled in PQ or in PV.

5.2.1 Controlled generator model

In the Newton MANA method presented in [28] and described hereinabove, all power generating devices are represented in the Jacobian as sets of constraint equations derived from their control settings. Each phase is modeled separately which yields 6 by 6 coefficient matrices for three-phase generators. Besides, additional terms ($\mathbf{B_{GI}}$, $\mathbf{B_{GE}}$ and $\mathbf{Y_G}$) are added in the Jacobian to account for generators' current constraint equations.

In the literature and in most commercial short-circuit analysis programs, the Type 4 WTG is generally represented as a voltage source behind impedance under abnormal conditions. The challenge in representing the Type 4 WTG as a Thevenin equivalent resides in the fact that the voltage angle and/or the impedance need to be iteratively adjusted to achieve the desired fault contribution [9], [26]. In the sub-transient operating mode, one doesn't know in advance the fault contribution of the WTG as it depends on several factors such as the pre-fault operating conditions and control operating set points. Therefore, as stated in [26], modeling the Type 4 WTG as a Thevenin equivalent wouldn't reproduce the real behavior of the WTG under fault conditions. Since the Thevenin equivalent model of the Type 4 WTG doesn't comply with the PQ controlled generator model limited in current, the Type 4 WTG cannot be represented as suggested in [28]. Instead, it is proposed to represent the full converter based WTG uniquely as a set of constraints derived according to its pre-fault control type, using matrices $\mathbf{J_p}$ and $\mathbf{J_{pI}}$. This representation is even extended to all type of controlled generators in [29], where it is assessed that for load flow calculations purposes, the Jacobian terms $\mathbf{B_{GI}}$, $\mathbf{B_{GE}}$ and $\mathbf{Y_G}$ are redundant as

long as the generators' control settings are adequately taken into account in the Jacobian through matrices $\mathbf{J_p}$ and $\mathbf{J_{pI}}$.

The same load-flow representation of constraints equations than presented in [28] is used for the purpose of modeling the Type 4 WTG under steady-state short-circuit operating conditions. It is important to clarify that, although the same load-flow representation of constraints equations as in [28] is used, a load flow is not run prior to the short-circuit calculations. The proposed model only accounts for the control mode that was set for the FCG prior to the fault. Short-circuit calculation is done with same traditional assumptions considering pre-fault voltage at 1 pu. Although not accurate, this is done to comply with the assumptions followed in CYME 7.0

Hence, for a PQ controlled WTG labeled as *p* and connected at an arbitrary node *k*, its constraint equations at a given iteration *j* are formulated as:

$$\mathbf{f_{GPQ}}^{j} = \begin{bmatrix} P_{des} - real\left(V_p.conj\left(I_p\right)\right) \\ Q_{des} - imag\left(V_p.conj\left(I_p\right)\right) \end{bmatrix}^{j} \tag{2.13}$$

where:

P_{des} : Desired (by-phase) active power of WTG *p*.

Q_{des} : Desired (by-phase) reactive power of WTG *p*.

I_p : Line current of WTG *p* connected to arbitrary node *k*.

V_p : Voltage of WTG *p* connected to arbitrary node *k*.

In this dissertation, it is assumed that the WTG is a three-phase device connected in Y/Yg configuration. Hence, V_p always refers to the line-to-neutral voltage of a WTG *p*.

Besides, the desired active and reactive power for each phase, P_{des} and $Q_{des,}$ are expressed as follows:

$$P_{des} = real\left(\frac{S_{des}}{3}\right) \tag{2.14}$$

$$Q_{des} = imag\left(\frac{S_{des}}{3}\right) \tag{2.15}$$

where:

S_{des} : Desired three-phase apparent power.

Formulation of the mismatch vector $\mathbf{f_{GPQ}}$ at iteration j as expressed in equation (2.13) can be rewritten as:

$$\mathbf{f_{GPQ}}^{j} = \begin{bmatrix} P_{des} - V_p^R I_p^R - V_p^I I_p^I \\ Q_{des} - V_p^I I_p^R + V_p^R I_p^I \end{bmatrix}^j \tag{2.16}$$

where:

R : Subscript which stands for the real part of the complex variable.

I : Subscript which stands for the imaginary part of the complex variable.

Equation (2.16) populates the Jacobian terms $\mathbf{J_{GPQ}}$ and $\mathbf{J_{GPQI}}$ which stand respectively for the voltage and current coefficient sub-matrices for the PQ controlled WTG. They are expressed as:

$$\begin{aligned} \mathbf{J_{GPQ}}^{j} &= \begin{bmatrix} -I_p^R & -I_p^I \\ I_p^I & -I_p^R \end{bmatrix}^j \\ \mathbf{J_{GPQI}}^{j} &= \begin{bmatrix} -V_p^R & -V_p^I \\ -V_p^I & V_p^R \end{bmatrix}^j \end{aligned} \tag{2.17}$$

For PV controlled generators, the voltage control is applied only on its magnitude and yields the mismatch vector $\mathbf{f_{GPV}}$ at iteration *j*, expressed as:

$$\mathbf{f_{GPV}}^{j} = \begin{bmatrix} P_{des} - V_p^R I_p^R - V_p^I I_p^I \\ V_{des} - \sqrt{\left(V_p^R\right)^2 + \left(V_p^I\right)^2} \end{bmatrix}^j \tag{2.18}$$

where:

P_{des} : Desired (by-phase) active power of WTG *p*.

V_{des} : Desired (by-phase) voltage of WTG *p*.

V_p : Voltage of WTG *p* connected to arbitrary node *k*.

I_p : Line current of WTG *p* connected to arbitrary node *k*.

Therefore, for a PV controlled generator labeled as *p* and connected to arbitrary node *k*, equation (2.18) yields the Jacobian term $\mathbf{J_{GPV}}$ which stands for the voltage coefficient sub-matrix in equation (2.8). $\mathbf{J_{GPV}}$ is expressed as:

$$\mathbf{J_{GPV}}^{j} = \begin{bmatrix} -I_p^R & -I_p^I \\ -\left[\left(V_p^R\right)^2 + \left(V_p^I\right)^2\right]^{-\frac{1}{2}} V_p^R & -\left[\left(V_p^R\right)^2 + \left(V_p^I\right)^2\right]^{-\frac{1}{2}} V_p^I \end{bmatrix}^j \tag{2.19}$$

Besides, according to the mismatch equation(2.18), the active power control yields additional Jacobian terms which represent the real and imaginary derivative of the generator's current $\mathbf{I_G}$. These terms can be regrouped in a sub-matrix $\mathbf{J_{GPVI}}$ expressed as:

$$\mathbf{J_{GPVI}}^{j} = \begin{bmatrix} -V_{km}^{R} & -V_{km}^{I} \\ 0 & 0 \end{bmatrix}^{j} \tag{2.20}$$

To stay consistent with the generic matrix formulation presented in [28] and shown in equation (2.8), the elements of sub-matrix $\mathbf{J_{GPVI}}$ should substitute the term $\mathbf{J_{GPQI}}$ provided that the Q row of the PQ control sub-matrix $\mathbf{J_{GPQ}}$ is replaced by the coefficients derived from the voltage constraint equation presented in (2.19).

5.2.2 Current limiting constraint

In the sub-transient operating mode, the maximum fault contribution of the Type 4 WTG is limited by the overload capability of the converter to which it is connected to. This is to protect the power converter from excessive fault currents that would damage the IGBT switches.

Therefore, at each iteration *j*, the fault current contribution provided by the sub-transient WTG model, I_{WTG}, is compared to the loading limits of the converter, $I_{VSC_\max}$. If I_{WTG} exceeds $I_{VSC_\max}$, the controlled generator model of the WTG is changed for a constant current source which value corresponds to the converter's threshold, $\mathrm{I}_{\mathrm{VSC_th}}$. $\mathrm{I}_{\mathrm{VSC_th}}$ is defined as :

$$I_{WTG_rated} \leq \mathrm{I}_{\mathrm{VSC_th}} \leq I_{VSC_\max} \tag{2.21}$$

where:

I_{WTG_rated} : Magnitude of rated current of the WTG.

$\mathrm{I}_{\mathrm{VSC_th}}$: Threshold current of the WTG's converter.

$I_{VSC_\max}$: Maximum current carrying capability of the WTG's converter (input data).

In this dissertation, the worst case scenario is considered, where:

$$\mathrm{I}_{\mathrm{VSC_th}} = I_{VSC_\max} \tag{2.22}$$

Typically, the maximum current carrying capability of the converter is set between 110% to 150% of the WTG rated current, depending on the cooling capabilities and the rating of the converter [25]. The magnitude of the converter's rated current, $\mathrm{I}_{\mathrm{WTG_rated}}$, is defined in equation(2.23) :

$$\mathrm{I}_{\mathrm{WTG_rated}} = \frac{S_{NOM}}{\sqrt{3}.V_{NOM}} \tag{2.23}$$

where:

V_{NOM} : Line-to-line rated voltage of the WTG.

S_{NOM} : Three-phase rated power of the WTG.

As for the angle of the converter's rated current, it is defined as:

$$\phi_{\mathrm{I}_{\mathrm{WTG_rated}}} = \cos^{-1}(PF_{NOM}) \tag{2.24}$$

Where:

PF_{NOM} : Power factor of the WTG at nominal value.

With the WTG modeled as an ideal current source, the mismatch vector $\mathbf{f_I}$ is expressed as:

$$\mathbf{f_I}^{j} = \begin{bmatrix} real(I_{des}) - real(I_p) \\ imag(I_{des}) - imag(I_p) \end{bmatrix}^{j} \tag{2.25}$$

where:

$$\mathrm{I}_{\mathrm{des}} = I_{VSC_\max} \tag{2.26}$$

Equation (2.25) yields the Jacobian term $\mathbf{J_I}$ which stands for the current coefficient sub-matrix for the current source. It is expressed as:

$$\mathbf{J_I}^{j} = \begin{bmatrix} -1 & 0 \\ 0 & -1 \end{bmatrix}^{j} \tag{2.27}$$

When the Type 4 WTG reaches the threshold of the converter and is modeled as a current source, the sub-matrix $\mathbf{J_I}$ replaces the term $\mathbf{J_{GPQI}}$ in the generic matrix equation (2.8). Besides, the term $\mathbf{J_{GPQ}}$ is null as, according to the mismatch vector shown in equation (2.25), there is no Jacobian term which represents the derivative of the PCC voltage.

5.3 Transient model

The Type 4 WTG can generally detect a default within 1 to 2 grid cycles after it occurs [25]. After fault detection, the Type 4 WTG operates in transient mode and its behavior changes. The WTG acts like a voltage dependent current source and, in practice, its fault contribution depends not only on the FRT requirements set by applicable grid codes but also on the inverter control strategy specific to each manufacturer.

With the increased wind penetration level in several countries, the wind turbine is required to remain connected to the grid during abnormal operating conditions to avoid affecting the grid stability. However, the amount of current to be injected by the WTG during fault ride through is not standardized yet and remains specific to each country. The fault current injection of the WTG can range from zero, i.e. no current injection, to the maximum current carrying capability of the converter [25]. In the absence of specific FRT requirements from national grid codes or utilities, WT manufacturers adopt their own control strategy to optimize the operation of the WTG. Since FRT specifications vary significantly among WTG manufacturers and so do they among national

grid codes, it is not possible yet to come up with a general behavior for the Type 4 WTG during transient operation regarding its fault contribution. Moreover, for the purpose of steady-state short-circuit analysis, it is impossible to assess the fault contribution of the WTG based on the control strategy implemented in the full-scale frequency converter. This latter relies on proprietary models which are generally not disclosed by WTG manufacturers. Besides, as stated in [25], such level of detail and complexity is usually not adopted in steady-state short-circuit studies. As a result, the only way to estimate the fault contribution of Type 4 WTG after fault detection is to assess the behavior of the WTG in accordance with applicable grid codes.

In this dissertation, the FRT requirements of the German grid code have been adopted [37]. Unlike other grid codes, it gives clear indication on the minimum amount of reactive current that needs to be injected to support the grid. Actually, Figure 5-1 shows the minimum reactive current that needs to be injected into the grid as a function of the voltage drop (or rise) at the PCC. This reactive current is in addition of the reactive current provided by the FCG before the fault. The required reactive current injection must start one cycle after the fault is detected, for voltage drops or rises larger than 10% of the WT nominal voltage.

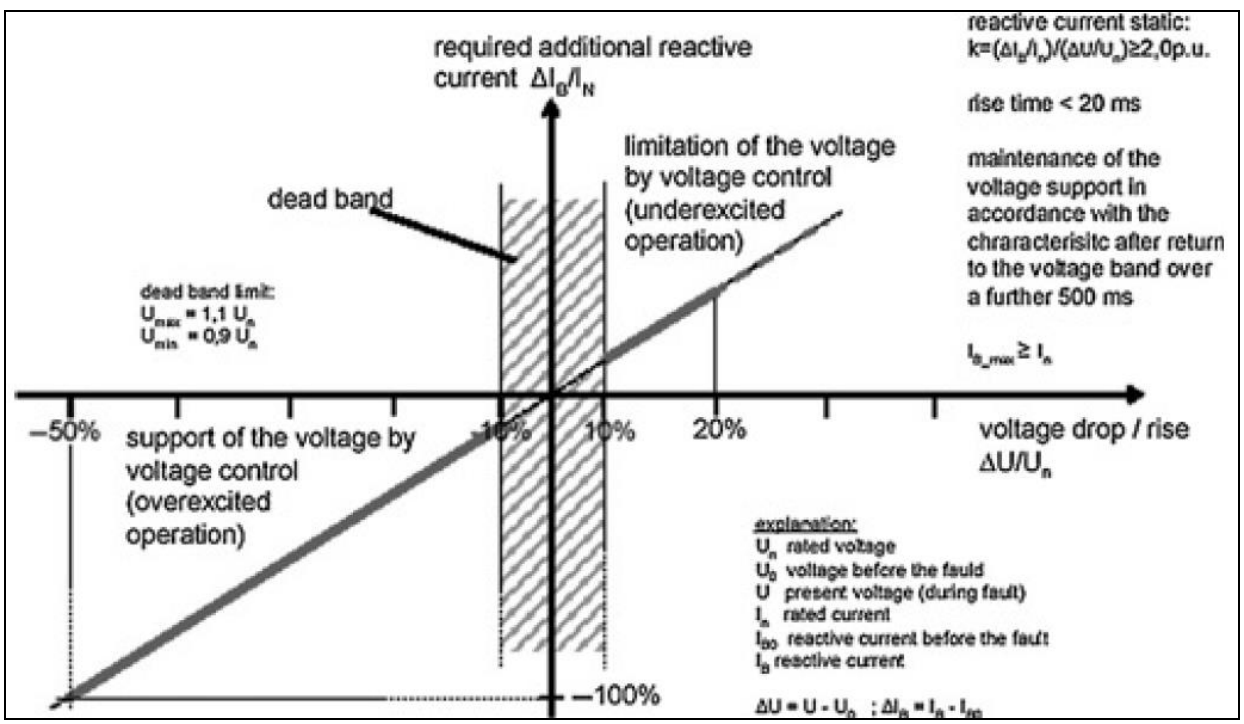

Figure 5-1 : Reactive current injection according to the German code [10].

In preponderant markets such as Germany or the province of Quebec, FRT requirements are based on the positive sequence voltage rather than the line to ground phase voltage [25]. Consequently, the additional reactive current to be injected also refers to the positive sequence value of the current. For an unsymmetrical fault, the reactive current injection is based on the maximum voltage drop (or rise) of all phases.

To reproduce the FRT requirements of Figure 5-1, the Type 4 WTG is modeled as a voltage controlled current source under transient operation.

The MANA formulation adopted for the sub-transient model of Type 4 WTG is used again for the transient model. In this case, the mismatch vector $\mathbf{f_I}$ is defined as:

$$\mathbf{f}_I^{\,j} = \begin{bmatrix} real\left(I_{des}\right) - real(I_p) \\ imag\left(I_{des}\right) - imag(I_p) \end{bmatrix}^j \tag{2.28}$$

where:

I_p : Line current of WTG *p* connected to arbitrary node *k*.

I_{des} : Desired current of WTG *p*.

In equation (2.28), the desired current refers to the phase current. It is expressed as:

$$I_{des} = \begin{bmatrix} 1 \\ a^2 \\ a \end{bmatrix} I_{1des} \tag{2.29}$$

where:

I_{1des} : Desired direct sequence current.

$$I_{1des} = I_{P1des} + jI_{Q1des} \tag{2.30}$$

In equation (2.30), the desired direct sequence reactive current I_{Q1des} is defined, in compliance with Figure 5-1, as:

$$I_{Q1des} = I_{Q10} + I_{Q1FRT} \tag{2.31}$$

Where:

I_{Q10} : Pre-fault direct sequence reactive current of WTG.

I_{Q1FRT} : Additional direct sequence reactive current required from WTG.

According to the German grid code, I_{Q1FRT} is determined as in Figure 5-1. It is function of the drop (or rise) of the PCC voltage during fault with respect to the PCC pre-fault voltage. As previously stated, in the German grid code, the voltage refers to the positive sequence voltage.

As for I_{P1des}, it generally depends on the proprietary models of WT manufacturers. Like stated in [25], most grid codes do not provide specific requirements regarding the active current injection during fault. An interesting alternative to determine the required active current injection is proposed in [9] and is consequently adopted in this dissertation with a slight but important difference. The worst case scenario is considered in the transient operating mode. Therefore, the WTG is assumed to contribute up to its maximum fault contribution rather than contributing up to the WTG's rated current. Hence, the desired active direct sequence current, I_{P1des}, is defined as:

$$I_{P1des} = \sqrt{I_{VSC_\max}^2 - I_{Q1des}^2} \tag{2.32}$$

This assumption is reasonable as long as the available wind power exceeds the WTG output power during the fault [31] and all WTG connected to a common full-scale frequency converter are considered in operation.

Equation (2.28) yields the Jacobian term $\mathbf{J_I}$ which stands for the current coefficient sub-matrix for the current source. At a given iteration *j*, it is expressed as:

$$\mathbf{J_I}^{j} = \begin{bmatrix} -1 & 0 \\ 0 & -1 \end{bmatrix}^{j} \tag{2.33}$$

The sub-matrix $\mathbf{J_I}$ is then integrated in the generic matrix equation (2.8).

In the province of Quebec, Hydro-Québec requires both synchronous and asynchronous generators connected to the grid to supply (or absorb) the reactive power corresponding to an overexcited (or underexcited) rated power factor equal to or less than 0.95 [32]. Such FRT requirement would be easy to implement in the multiphase MANA formulation adopted. Indeed, one could deduct the desired active and reactive current to be injected in the grid considering the maximum power factor, i.e. 0.95, and the maximum fault contribution.

5.4 Short-circuit algorithm

5.4.1 Short-circuit calculation methods

Short-circuit analysis is performed using either sequence network representation or detailed multiphase representation. Traditionally, the symmetrical component formulation was preferred as it provided a convenient and trivial way of representing unsymmetrical faults in a balanced system in accordance with Fortescue's theorem. The nodal admittance matrix method (Y_{Bus}), the nodal impedance matrix method (Z_{Bus}) and the classical nodal analysis method are other methods that can be used for formulating network equations for short-circuit calculations. However, they present significant limitations regarding the modeling of complex transformer connections, ungrounded voltage sources, ideal current sources and zero impedance devices [33].

The modified-augmented-nodal-analysis (MANA), presented in [28] as the most general approach available in literature, overcomes all the shortcomings aforementioned and follows a formulation method of network equations which allows handling arbitrary network topologies along with various component models. Nowadays, with the proliferation of fast computers with large core memory, it is more advantageous to use actual multiphase representation since it provides more accurate modeling capabilities. Yet, thanks to modern sparse matrix techniques, the method can be easily implemented without compromise on the solution's performance; even for large distribution systems [34]. As a result, the method proves to be very well adapted to model North American distribution networks which are inherently unbalanced and are characterized by their single and double phase laterals topology. Moreover, the necessity to address new modeling challenges like the connection of distributed generation to the distribution system or the detailed modeling of unusual transformer topologies further justifies the benefits of using a phase domain analysis approach [34]. While sequence network representation requires special treatment of unusual configurations and could possibly lead to significant errors in short-circuit studies, the generic multiphase formulation provides a general approach to handle arbitrary network topologies and accurately model various devices [28], [34], [35].

Due to the nature of the proposed models of Type 4 WTG, the MANA formulation is used in this dissertation as it is the only short-circuit method which allows representing ideal current sources directly. Besides, the MANA formulation [28] [44] has proven to be the most systematic and efficient approach to model controlled devices by accommodating arbitrary equations like constraint equations.

5.4.2 MANA shunt fault models

In the MANA formulation, faults are represented by ideal switches. As presented in [33], only sub-matrices $\boldsymbol{S_c}$ and $\boldsymbol{S_d}$ from equations (2.9) and (2.11) are modified to insert fault equations, thus avoiding manipulating the existing network or renumbering the Jacobian matrix. Fault impedances Z_f and Z_g are also taken into account in these sub-matrices. The most common types of faults are represented in Figure 5-2 which is taken from [33].

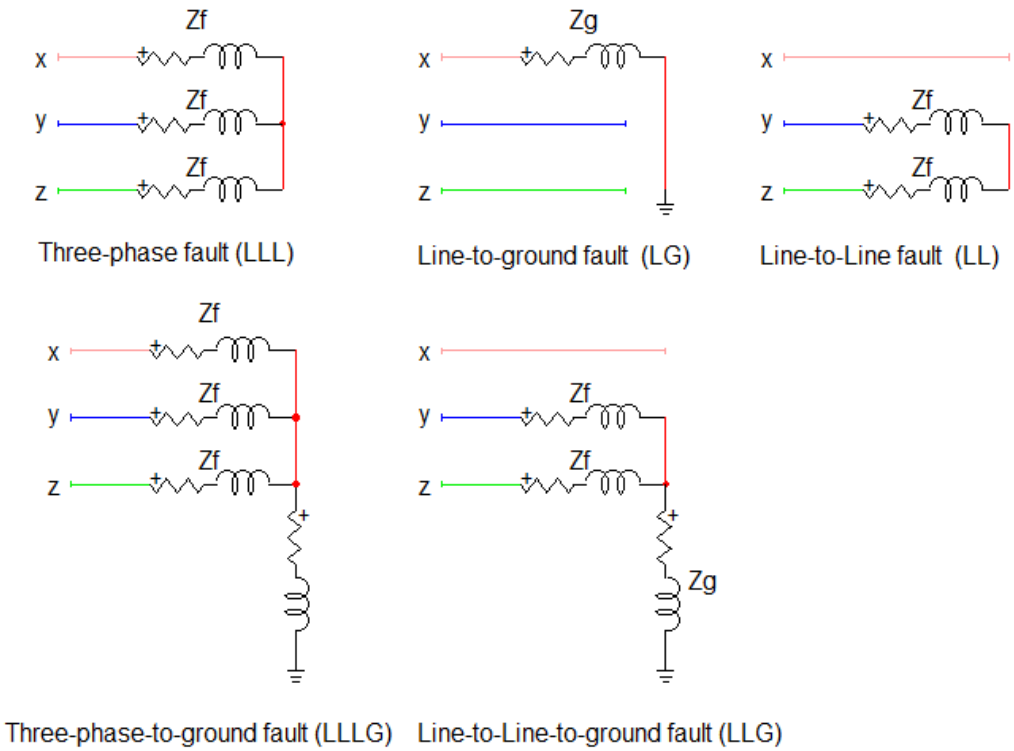

Figure 5-2 : Shunt Fault Representation with Impedance [33]

The formulation of matrices $\boldsymbol{S_c}$ and $\boldsymbol{S_d}$ depends on the type of fault that is represented. For example, the MANA model of a single line-to-ground (LG) fault is represented in Figure 5-3 and yields equation (2.34) [33].

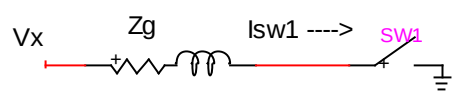

Figure 5-3 : MANA LG Fault Model

$$V_x - Z_g I_{SW1} = 0 \tag{2.34}$$

where:

V_x : Fault voltage on phase x.

Z_g : Fault impedance.

I_{SW1} : Fault current.

Consequently, for a LG fault on phase x, matrices $\mathbf{S_c}$ and $\mathbf{S_d}$ are expressed as [33]:

$$\mathbf{S_c} = [\mathbf{1}] \tag{2.35}$$

$$\mathbf{S_d} = [\mathbf{-Z_g}] \tag{2.36}$$

The MANA model of a three-phase (LLL) fault is represented in Figure 5-4 and yields equation (2.37).

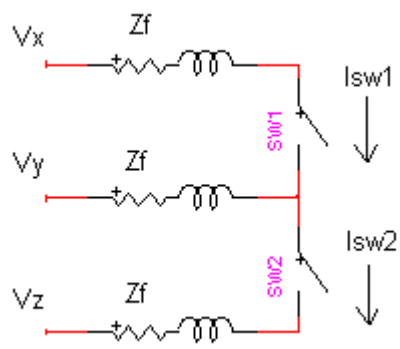

Figure 5-4 : MANA LLL Fault Model [33]

$$V_x - V_y - 2Z_f I_{SW1} + Z_f I_{SW2} = 0 \tag{2.37}$$

$$V_y - V_z - 2Z_f I_{SW2} + Z_f I_{SW1} = 0 \tag{2.38}$$

Consequently, for a LLL fault, matrices $\mathbf{S_c}$ and $\mathbf{S_d}$ are expressed as [33]:

$$\mathbf{S_c} = \begin{bmatrix} 1 & 0 \\ -1 & 1 \\ 0 & -1 \end{bmatrix} \tag{2.39}$$

$$\mathbf{S_d} = \begin{bmatrix} -2Z_f & Z_f \\ Z_f & -2Z_f \end{bmatrix} \tag{2.40}$$

Detailed representation of other types of fault can be found in [33].

5.4.3 Fault flow algorithm

5.4.3.1 Short-circuit calculations assumptions

In the proposed MANA-based fault flow algorithm, all devices other than the Type 4 WTG are modeled as linear devices based on the short-circuit MANA representation, as detailed in [33]. In particular, all generators except inverter connected generators are modeled as voltage source behind impedance. The value of the impedance can be the sub-transient, transient or steady-state value depending on the period studied.

Besides, same assumptions as in traditional short-circuit analysis are made to have the same basis of comparison later on, when comparing the existing short-circuit models of Type 4 WTG with the proposed one. As a result, loads, shunt capacitors and line charging effects are neglected, pre-fault voltages are considered nominal and transformers are set at nominal tap.

Since loads are neglected, the generic matrix equation (2.8) yields:

$$\begin{bmatrix} \mathbf{Y_n} & \mathbf{A_c} & \mathbf{A_{IG}} \\ \mathbf{A_r} & \mathbf{A_d} & \mathbf{0} \\ \mathbf{J_G} & \mathbf{0} & \mathbf{J_{GI}} \end{bmatrix}^j \begin{bmatrix} \mathbf{\Delta V_n} \\ \mathbf{\Delta I_x} \\ \mathbf{\Delta I_G} \end{bmatrix} = -\begin{bmatrix} \mathbf{f_n} \\ \mathbf{f_x} \\ \mathbf{f_G} \end{bmatrix}^j \tag{2.41}$$

Although it has been chosen to neglect loads, shunt capacitors and line charging effects, it is important to mention that the Jacobian matrix formulation proposed in [28] allows accurately representing these elements for short-circuit calculations purposes. Therefore, for more precision, they could be modeled in the Jacobian matrix in equation (2.41). In such case, loads would be modeled as constant impedances rather than being modeled according to their PQ constraint equations. As for pre-fault voltages, they can also be considered at load-flow value instead of nominal value for more precision.

5.4.3.2 Initialization of fault flow algorithm

Since the solution of the matrix equation (2.41) is found based on the Newton method, suitable initialization of the algorithm is crucial to guarantee the convergence and performance of the method. For this reason, the proposed fault flow algorithm is initialized with the Fixed-Point MANA method presented in [28]. All devices are represented as linear devices. They are modeled according to their MANA short-circuit model detailed specifically for each equipment in [33]. As for the Type 4 WTG, it is proposed to model it as a three-phase voltage source behind constant impedance. Each phase is modeled separately and yields equations (2.42) and (2.43) below:

$$E_{WTG} = V_{NOM_LN} \tag{2.42}$$

$$Z_{WTG} = \frac{V_{NOM_LN}}{I_{VSC_th}} \tag{2.43}$$

where:

V_{NOM_LN} : Nominal line-to-neutral voltage of the WTG (V).

I_{VSC_th} : Threshold current of the WTG's converter defined as in equation (2.22) (A).

The matrix equation (2.44) is then solved in a single iteration of the fixed point method as proposed in [29]. As explained hereinabove, faults are represented by ideal switches and represented in sub-matrices $\mathbf{A_c}$, $\mathbf{A_r}$ and $\mathbf{A_d}$.

$$\begin{bmatrix} \mathbf{Y_n} & \mathbf{A_c} \\ \mathbf{A_r} & \mathbf{A_d} \end{bmatrix} \begin{bmatrix} \mathbf{\Delta V_n} \\ \mathbf{\Delta I_x} \end{bmatrix} = -\begin{bmatrix} \mathbf{f_n} \\ \mathbf{f_x} \end{bmatrix} \tag{2.44}$$

In its compact form, matrix equation (2.44) yields:

$$\mathbf{AX} = \mathbf{b} \tag{2.45}$$

The mismatch between the linear solution obtained from the fixed-point solution and the sought final solution will depend on the control operating set-points and the distance-to-fault of the WTG. By modeling the Type 4 WTG according to its maximum fault contribution at the initialization step, the solution of the fixed-point algorithm is very close to the final solution for faults close to the WTG. As for remote faults, more iterations are necessary to reach the final solution. Besides, since all devices other than the Type 4 WTG are modeled appropriately, the fixed point allows obtaining a solution very close to the final one in a single iteration. Figure 5-5 shows the initialization routine described and adapted from [29].

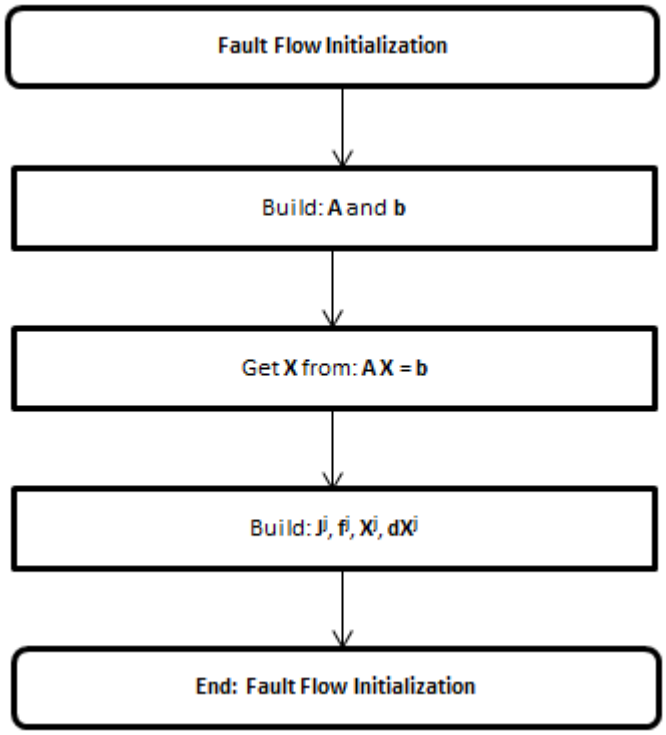

Figure 5-5 : Initialization of the fault-flow algorithm.

5.4.3.3 Fault flow algorithm

The MANA approach used in [28] to build the Jacobian matrix allows adopting a systematic and yet efficient method to integrate into the Jacobian such arbitrary equations like constraint equations as it allows partitioning the latter into matrices which contain all the devices without controls and the remaining block matrices which represent the controlled devices. Devices without controls are modeled as in the classical MANA formulation throughout sub-matrices Yn, Ar, Ac and Ad. As for controlled devices, they are represented in the Jacobian according to their control type.

Consequently, the generic matrix equation presented in equation (2.44) and used to initialize the Newton-based fault-flow algorithm doesn’t need to be modified. It is simply augmented with the constraint equations relevant to the pre-fault control strategy applied to the Type 4 WTG, yielding matrix equation (2.41).

The MANA approach applied to short-circuit analysis is generally not iterative and a single factorization step is enough to find the solution. However, in this dissertation, we have assessed that both the sub-transient and transient models of Type 4 WTG need to be adjusted iteratively. Hence, to accommodate the iterative nature of the WTG model developed, the Newton method presented in [28] is adapted to perform fault flow analysis. The Jacobian is iteratively updated with the adjusted model of WTG until the mismatch equation is minimized within the specified tolerance. In this iterative process, only the mismatch vector $\mathbf{f_p}$ and the sub-matrices $\mathbf{J_p}$ and $\mathbf{J_{pI}}$ which represent the constraint equations are updated. The solution provides the fault current contribution of Type 4 WTG according to their real behavior under fault conditions. Figure 5-6 and Figure 5-7 describe the proposed fault-flow algorithm which is adapted from [29].

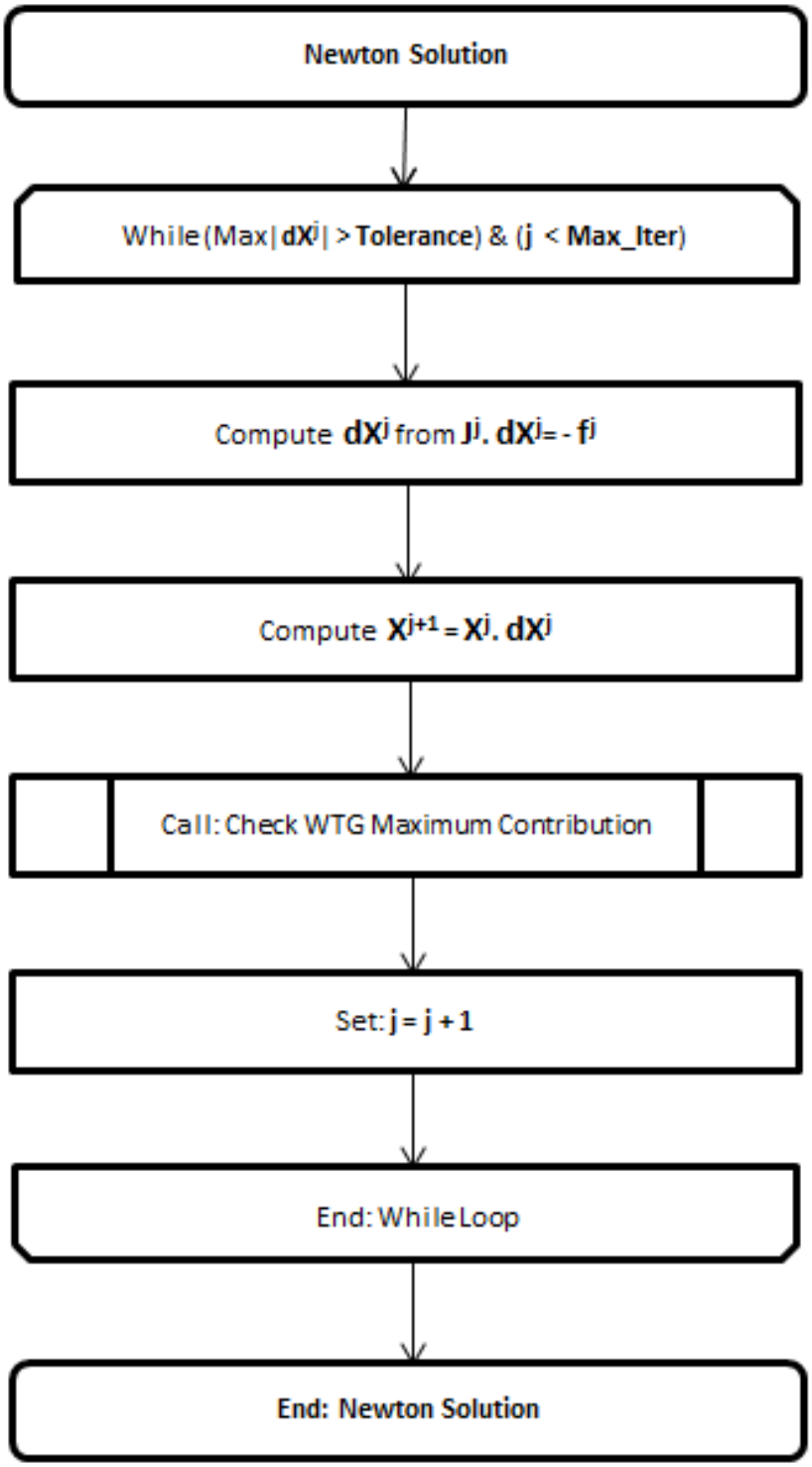

Figure 5-6 : Fault-flow algorithm

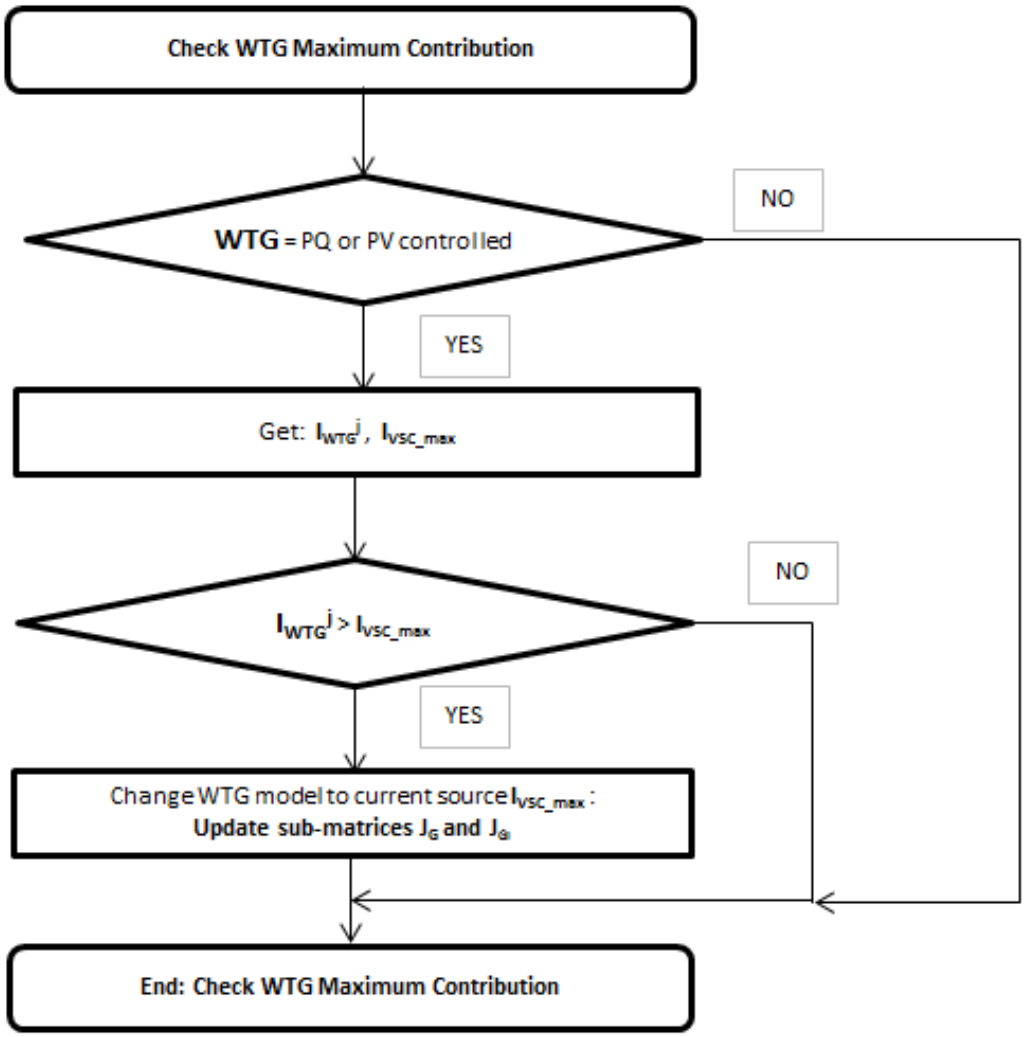

Figure 5-7 : Algorithm to check the WTG maximum fault contribution.

CHAPITRE 6 MODEL VALIDATION

6.1 Validation of the new model against detailed EMTP model

6.1.1 Description of the study network

The network studied is the same as in Chapter 3, i.e. a 1x2 MW (2.22 MVA) wind turbine generator connected to a 34.5kV Distribution System at the Point of Common Coupling (PCC) through a 2.5 MVA, 0.575/34.5 kV step-up transformer. The single-line diagram of the benchmark network is reproduced in Figure 6-1.

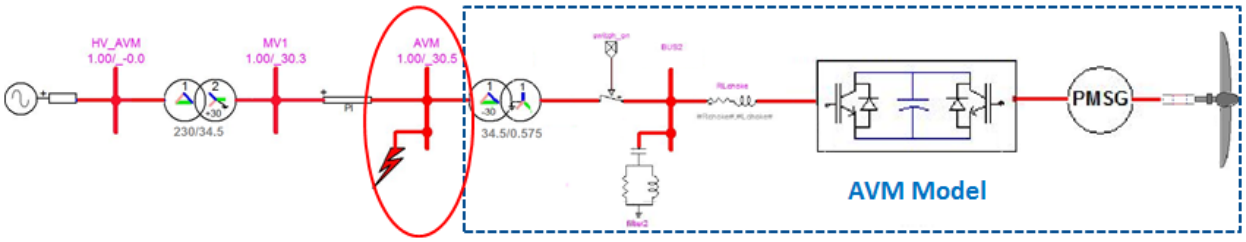

Figure 6-1: Single-line diagram of the benchmark network

Three phase (LLL) fault and single line-to-ground (LG) fault are respectively applied at the HV-AVM bus which is also considered to be, in practice, the point of common coupling (PCC) of the wind turbine to the grid.

However, as discussed in Chapter 3, to validate the model of FCG developed, we will compare the current contribution of the detailed EMTP-RV model and the proposed model at the LV side of the FCG's step-up transformer instead of comparing the fault contribution of the two models at the HV-AVM bus. This is because, in CYME 7.0 where the proposed model is meant to be implemented, the FCG model doesn't include either the step-up transformers or the collector line. These types of equipment are modeled separately.

6.1.2 Results and discussion

6.1.2.1 LG fault at the HV-AVM bus

A single line-to-ground fault is applied at the HV-AVM bus. The value of the fault impedance is varied from 0 to 120 ohms to simulate a wide range of voltage drop at the LV side of the FCG's step-up transformer. The fault contribution obtained with the detailed model of EMTP-TV is compared with the fault contribution provided by the proposed model. Since the contribution provided by the detailed model in EMTP-RV varies with time, the maximum contribution observed during the fault period has been considered for the comparison. Results obtained are shown in Figure 6-2.

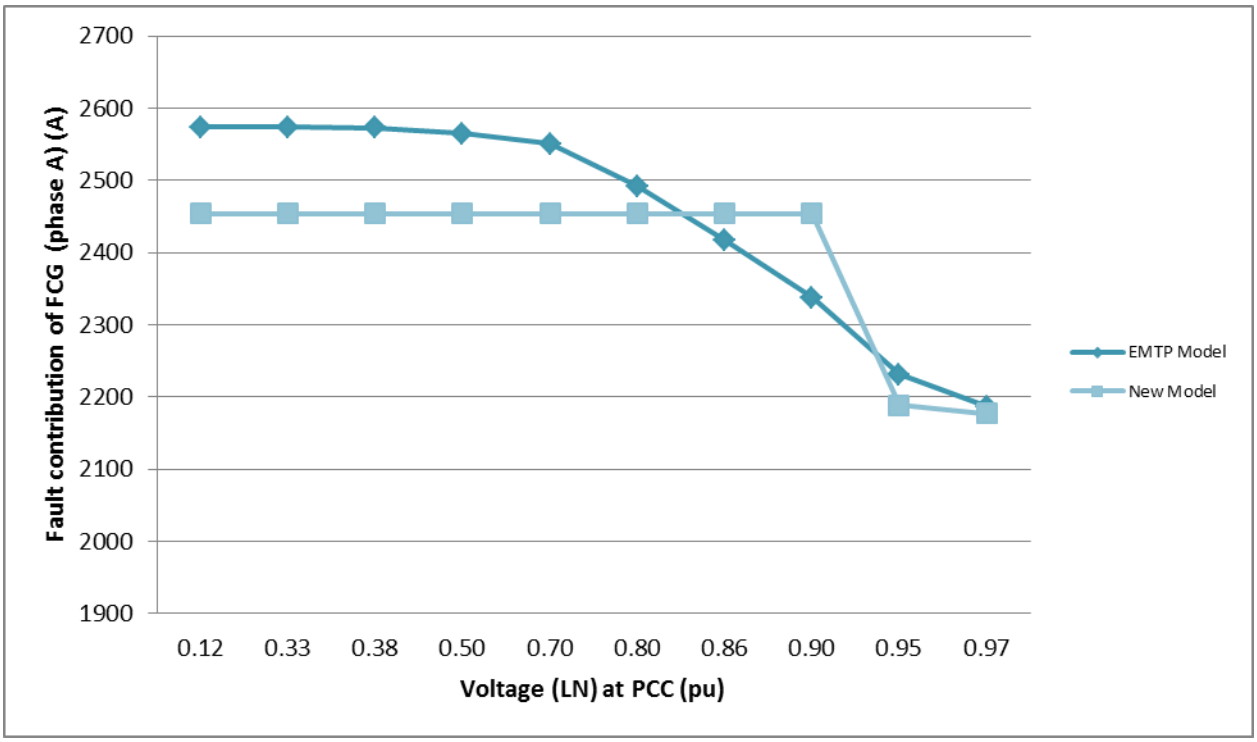

Figure 6-2 : Fault contribution of the FCG for a LG fault

As shown in Figure 6-2, the fault contribution provided by the detailed EMTP model is different from the fault contribution provided by the new model.

With the detailed EMTP-RV model, the fault contribution of the FCG decreases as the voltage drops at the LV side of the FCG's step-up transformer. As shown in Chapter 3, the fault current contribution of the FCG is determined by the response of the PI controller in accordance with the reactive power control mode selected. The fault contribution of the FCG never exceeds the limit set by the current limiter.

With the proposed model, the FCG consistently injects the maximum current contribution of the VSC up to 10% voltage drop at the LV side of the FCG's step-up transformer. For the validation purposes, the overload capability of the VSC has been set at 110% of the rated current of the WTG. When the voltage drop at the LV side of the FCG's step-up transformer is less than 10%, the fault contribution of the proposed model decreases to values close to the pre-fault current contribution.

The difference between the EMTP detailed model and the proposed model mainly comes from the difference in the control strategy applied. In EMTP a reactive control mode is selected for which the reactive power reference (Qref_pu) is zero. Besides, the WTG doesn't provide any active power during the fault. However, with the proposed model, the FCG hits the maximum current contribution of the VSC and behaves like a constant current source as it cannot sustain the required PQ constraints resulting from the control strategy set prior to the fault.

Besides, for the detailed EMTP-RV model, the converter's current limiter is referenced in the dq0 frame whereas, with the proposed model, it is limited in the phase domain. This yields the difference observed in the maximum fault contribution provided by the detailed EMTP model and the proposed model.

6.1.2.2 LLL fault at the HV-AVM bus

A three-phase fault is applied at the HV-AVM bus. The value of the fault impedance is varied from 0 to 120 ohms to simulate a wide range of voltage drop at the LV side of the FCG's step-up transformer. The fault contribution obtained with the detailed model of EMTP-TV is compared with the fault contribution provided by the proposed model. Since the contribution provided by the detailed model in EMTP-RV varies with time, the maximum contribution observed during the fault period has been considered for the comparison. Results obtained are shown in Figure 6-3.

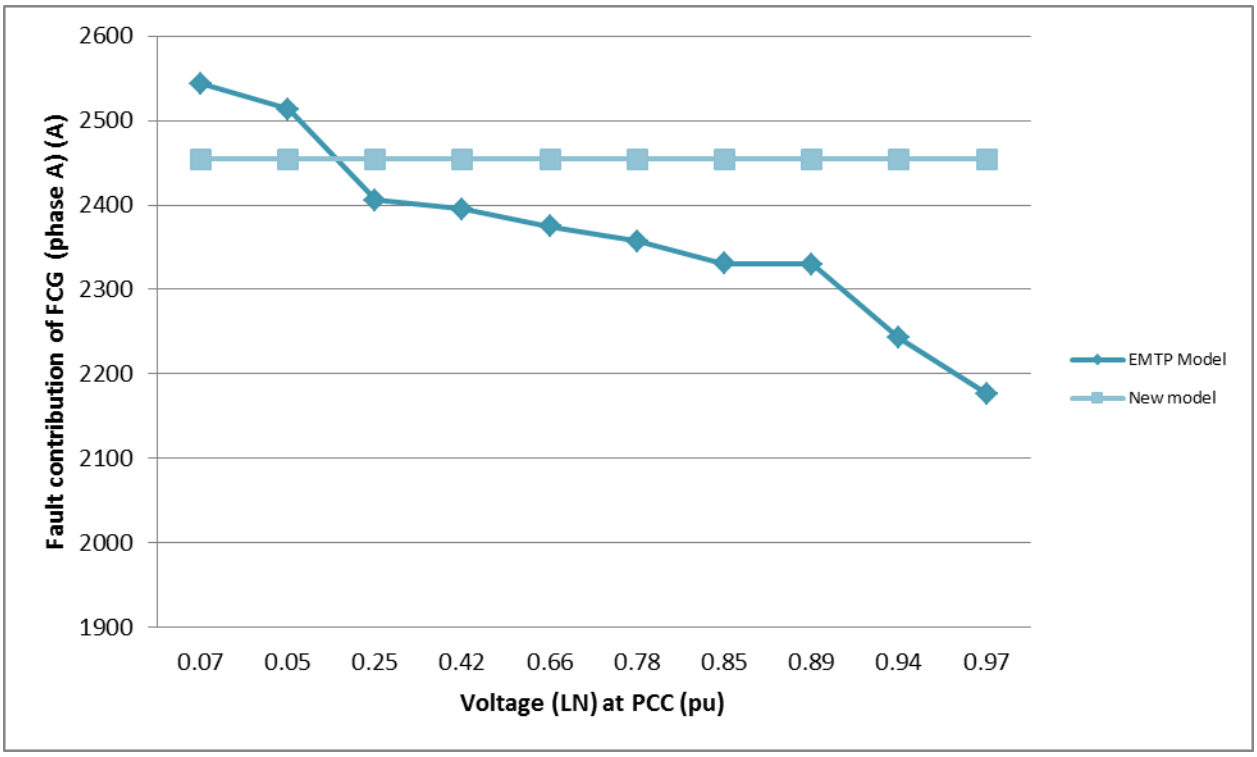

Figure 6-3 : Fault contribution of the FCG for a LG fault

Like for the LG fault, Figure 6-3 shows that the fault contribution provided by the detailed EMTP model is different from the fault contribution provided by the new model.

With the detailed EMTP-RV model, the fault contribution of the FCG decreases as the voltage drops at the LV side of the FCG's step-up transformer. Once again, the fault current contribution of the FCG is determined by the response of the PI controller in accordance with the reactive power control mode selected. The fault contribution of the detailed EMTP-RV model is also limited under the pre-set value of the converter's current limiter.

With the proposed model, the FCG consistently injects the maximum current contribution of the VSC, i.e. 110% of the rated current of the WTG, regardless of the voltage drop at the LV side of the FCG's step-up transformer. It therefore behaves like a constant current source.

Similarly to what was observed for the LLL fault, the difference between the EMTP detailed model and the proposed model mainly comes from the difference in the control strategy applied

along with the difference in the reference frame considered to limit the current carrying capability of the converter.

6.2 Comparison of the new model with the models in CYME 7.0

In this section, we will compare the proposed model with the current models in CYME 7.0.

6.2.1 Description of the study network

The network used to validate the proposed model of FCG developed for short-circuit steady-state calculations is the Fortis Alberta 25 kV distribution system. An equivalent representation of this network is presented in Figure 6-4.

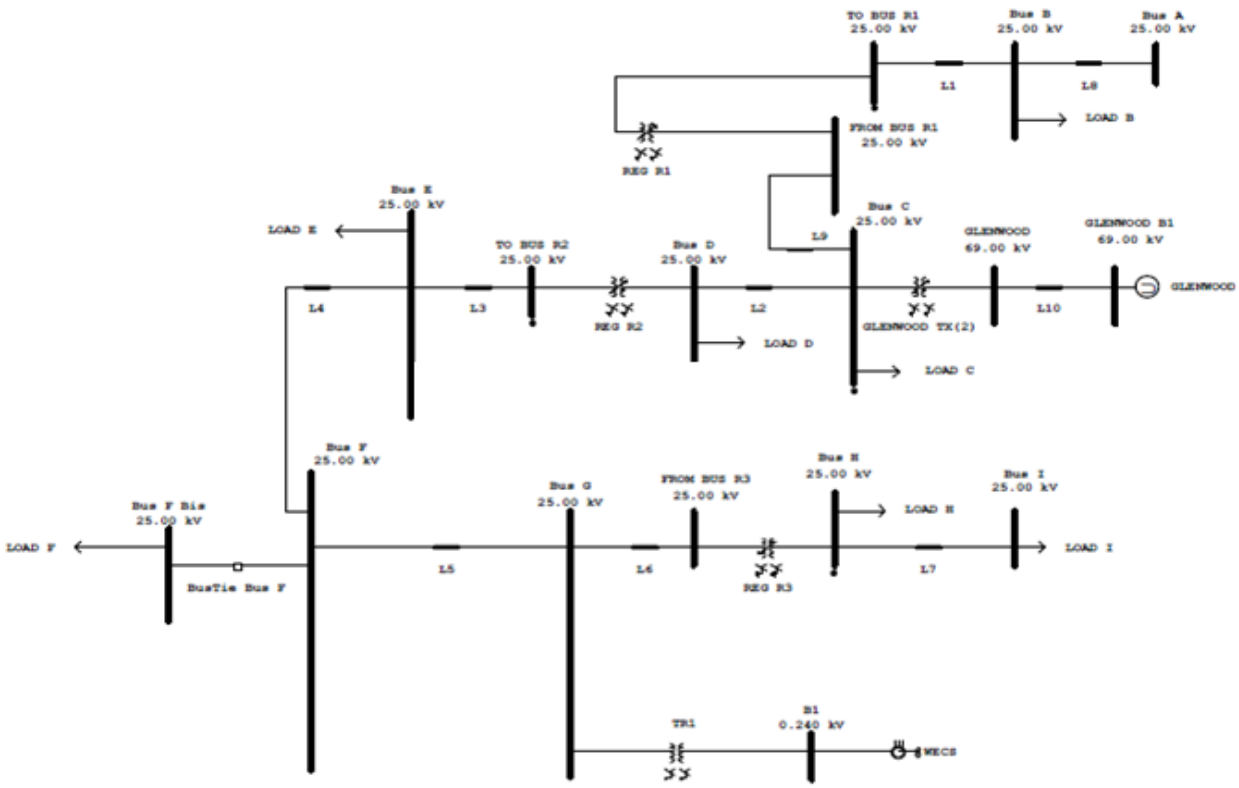

Figure 6-4: Equivalent representation of Fortis Alberta 25 kV distribution system.

The distribution system is connected to the main 69 kV power system at Glenwood Substation bus bar “Glenwood”. The 69 kV grid has a three-phase short-circuit capacity of 260 MVA and a

single-phase short-circuit capacity of 181 MVA. Its X1/R1 ratio is 1.602 and its X0/R0 ratio is 3.069.

A FCG of 436.5 kW, 0.24 kV is connected to bus bar 147-0. Its converter is designed with an overload capability of 20% above rated, hence 1260.07 A. Loads are connected to bus bars B, C, D, E, F, H and I. Their contribution is however neglected in the short-circuit analysis.

6.3 Fault contribution of Type 4 WTG under various fault conditions

This section discusses the results obtained for LLLG and LG faults, applied respectively at different buses, for different pre-fault conditions and assuming that the WTG operates in fixed generation mode prior to the fault. For each scenario, the WTG fault contribution obtained with the proposed model is compared with results from CYME, considering both a nominal pre-fault voltage (column CYME NOMINAL in the tables below) and a pre-fault voltage (column CYME LOAD FLOW in the tables below) computed from the load flow solution.

6.3.1 Three-phase fault at various locations

6.3.1.1 Desired active generation: 436.5 kW

A three-phase fault is applied at different buses of the distribution network. Prior to the fault, the Type 4 WTG operates in fixed generation mode and its desired active generation is set to 436.5 kW, which corresponds to the rated power of the generator. Figure 6-5 shows the resultant fault contribution of the WTG.

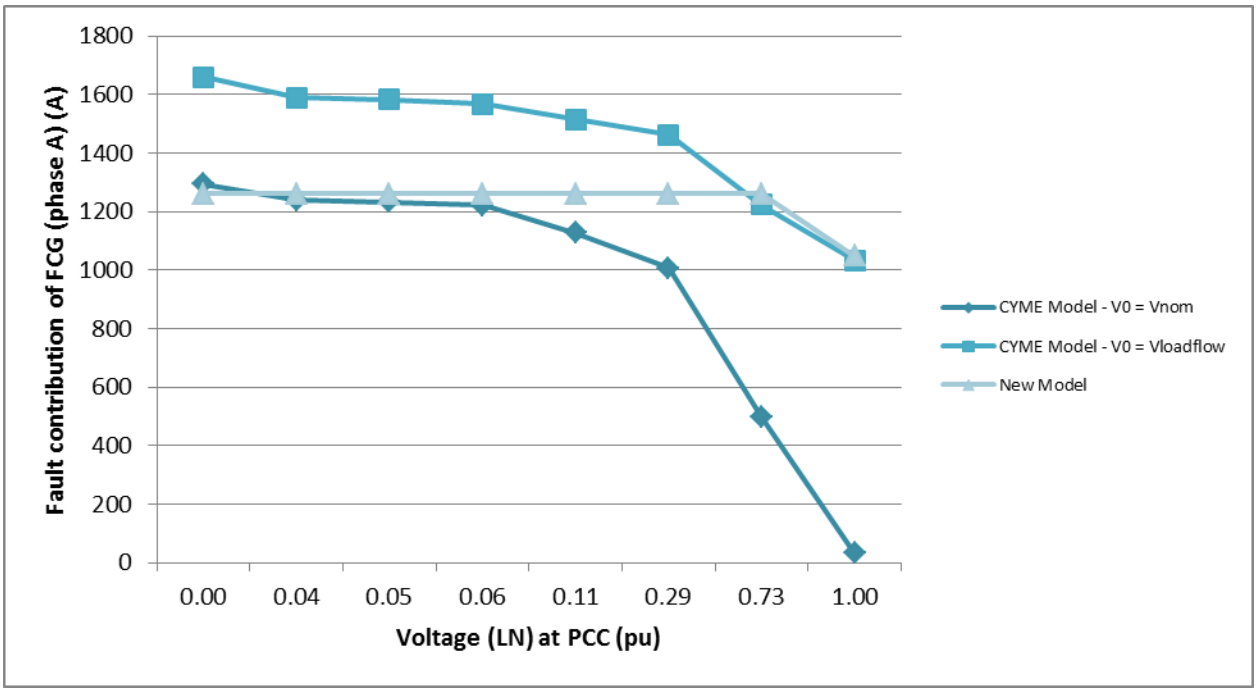

Figure 6-5: Fault contribution of Type 4 WTG for LLL fault – Pdes = 436.5 kW

With the new model, as shown in Figure 6-5, the Type 4 WTG contributes to its maximum value, up to 27% of voltage drop at the PCC, when a three-phase fault occurs on BUS_A. This behavior is expected since the WTG operates at its rated power prior to the fault. Besides, the converter overload capability is only 1.2 times the rated current of the WTG, i.e. 1260.07 A. Therefore, there is almost no margin to possibly maintain the desired active generation without reaching the converter's threshold. For a remote fault located on bus 96, there is almost no voltage drop at the PCC. Therefore, the fault contribution of the WTG results from the set desired active generation.

Results from Figure 6-5 also show that, in CYME 7.0, the actual models of WTG don't account for the overload capability of the converter since fault contributions up to 1.3 times higher than the admissible limit of the converter have been estimated. Additionally, based on the WTG fault contribution calculated for a remote fault on bus 96, it is clear that the current models of FCG in CYME 7.0 also don't reflect the control mode applied prior to the fault.

Finally, comparison of the fault contribution of Type 4 WTG from CYME 7.0 and the proposed model show that, when nominal pre-fault voltage is assumed, the fault contribution of the FCG is significantly underestimated, especially for remote faults where, in the studied case, the fault

contribution of the WTG has been underestimated by 97% . As for when load flow pre-fault conditions are assumed, the fault contribution of the Type 4 WTG is generally overestimated. The worst case is at the PCC where CYME 7.0 models provide fault contribution up to 30% higher than the proposed model.

6.3.1.2 Desired active generation: 150 kW

The pre-fault operating conditions of the FCG are changed and the WTG desired active generation is lowered to 150 kW. Figure 6-6 compares the fault contribution of the FCG based on the proposed model and actual models in CYME 7.0.

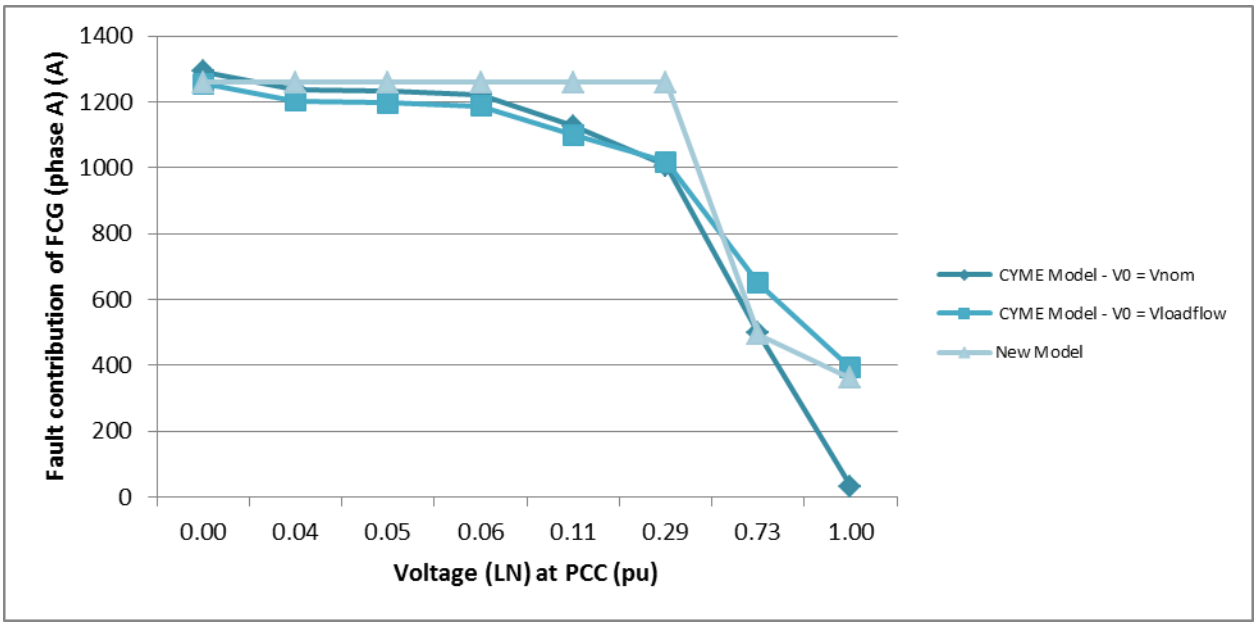

Figure 6-6 : Fault contribution of Type 4 WTG for LLL fault – Pdes = 150 kW

In the case studied, for a three-phase fault, starting at lower desired active generation doesn't affect the fault contribution of the WTG which still generates a maximum fault contribution up to when the fault is located on BUS_A. However, the impact of the lower desired active generation shows for remote faults, for which the Type 4 WTG is modeled as a set of negative PQ constraints and its current contribution is determined accordingly.

As for the fault contributions obtained from the CYME 7.0 models, as noted previously, they don't reflect neither the overload capability of the converter in case of a close default, nor the constraints set by the pre-fault control mode in case of remote faults.

6.3.2 Line-to-ground fault at various locations

6.3.2.1 Desired active generation: 436.5 kW

A line-to-ground fault is applied at different buses of the distribution network.

Prior to the fault, the Type 4 WTG operates in fixed generation mode and its desired active generation is set to 436.5 kW, which corresponds to the rated power of the generator. Figure 6-7 shows the resultant fault contribution of the WTG.

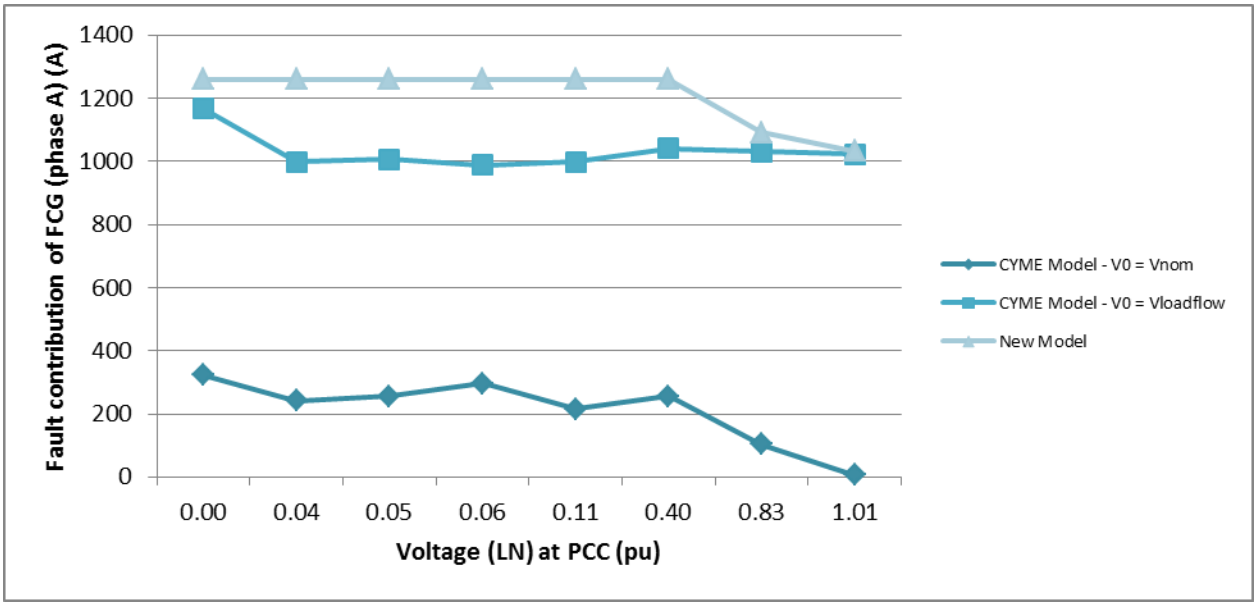

Figure 6-7 : Fault contribution of Type 4 WTG for LG fault – Pdes = 436.5 kW

Like for the case of a three-phase fault, Figure 6-7 shows that the contribution of the Type 4 WTG is maximal at several locations in the distribution network. For remote faults, the contribution of the WTG, subsequent to the line-to-ground fault, is in accordance with the pre-fault desired active generation.

As for the fault contribution obtained from the CYME 7.0 models, they show, as mentioned before that neither the overload capability of the, nor the pre-fault control mode are taken into account in determining the fault contribution of the Type 4 WTG.

Comparison of the fault contribution of Type 4 WTG from CYME 7.0 and the proposed model show that, for a default at the PCC, CYME 7.0 models underestimates the fault contribution of the Type 4 WTG on the faulted phase both when load flow pre-fault conditions or nominal pre-fault conditions are assumed.

For remote faults, the fault contribution obtained when load flow pre-fault conditions are assumed are close to the fault contribution of the proposed model, but yet, don’t reflect the control mode applied under steady-state conditions. As for when nominal pre-fault conditions are assumed, the fault contribution from the CYME 7.0 models is significantly underestimated.

6.3.2.2 Desired active generation: 150 kW

The pre-fault operating conditions of the Type 4 WTG are changed and the WTG desired active generation is lowered to 150 kW. Figure 6-8 compares the fault contribution of the Type 4 WTG based on the proposed model and actual models in CYME 7.0.

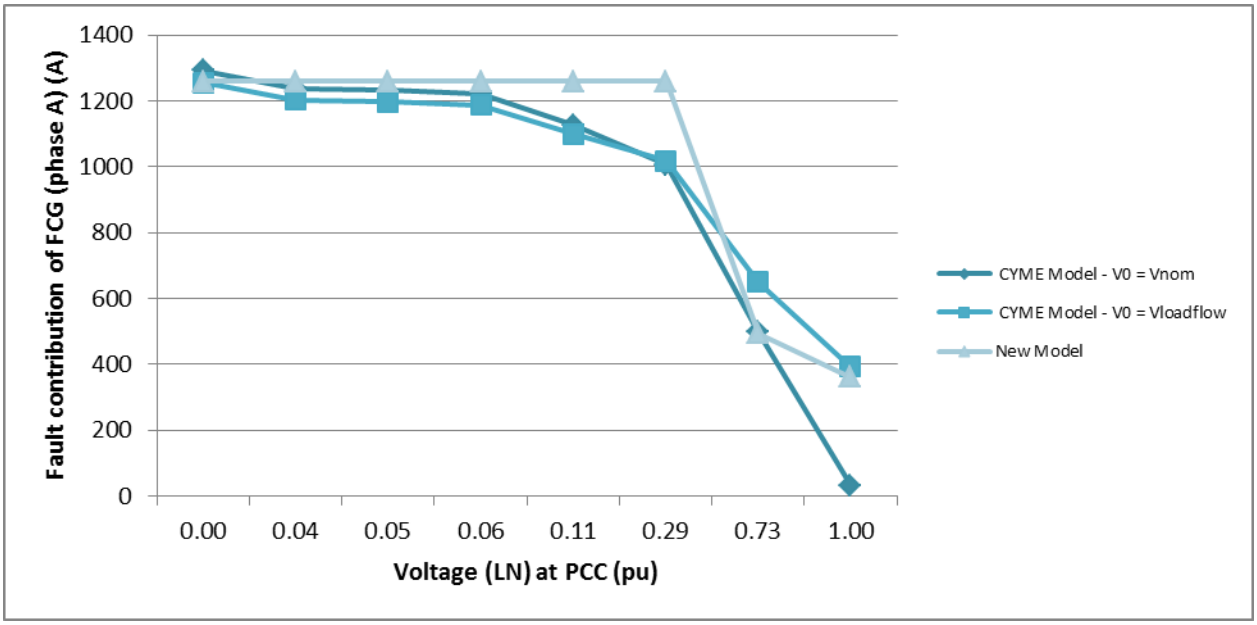

Figure 6-8 : Fault contribution of Type 4 WTG for LG fault – Pdes = 150 kW

The results in Figure 6-8 show that for a line-to-ground fault and pre-fault conditions lower than rated values, the fault contribution provided by the CYME 7.0 model when load-flow pre-fault conditions are assumed is slightly higher than the fault contribution found with the proposed model. However, the fault contribution from the CYME 7.0 model which assumes nominal pre-fault conditions is still significantly underestimated.

CONCLUSION

Actual representation of FCG in commercial short-circuit analysis software tools doesn't reproduce their real behavior under steady-state fault conditions. Actually, most packages don't allow direct representation of current sources since they use sequence network representation to perform short-circuit calculations [38]. As a result, Type 4 WTG is modeled as a voltage source behind impedance which is iteratively adjusted to match the fault current contribution of the WTG. This model is not appropriate, especially in sub-transient operating mode for which one cannot determine in advance the fault contribution of the WTG. In CYME [41], the value of this impedance is fixed and is derived from a three-phase bolted fault at the WTG terminals. As a result, at nominal pre-fault voltage, the mismatch between the WTG's fault current contribution computed by CYME and the WTG's real fault contribution increases with the distance from PCC to fault. Besides, in CYME, the Type 4 WTG is assumed to inject only reactive current into the grid whereas, in practice, the currents injected by a Type 4 WTG have real and reactive components as determined by the applicable grid code minimum LVRT requirements [26].

The purpose of this research work was to provide a simple model of Type 4 WTG which closely reproduces its real behavior under fault conditions. However, comparison with the detailed EMTP model shows that the proposed model doesn't provide the same fault contribution than the detailed EMTP model under similar fault conditions. The difference observed between the two models mainly results from the difference in the control strategy applied during the fault. Actually, in EMTP, the FCG is controlled to stop delivering active power during the fault and to either inject reactive power into the grid (Q control) or also support the grid voltage (Q+Vac control). However, with the proposed model, the fault contribution of the FCG depends on the control strategy set prior to the fault and the FCG tends to behave like a constant current source as a result of the voltage drop at the LV side of the FCG's step-up transformer. On the other hand, for remote faults, the proposed model operates close to its pre-fault values. Besides, the difference observed between the two models is also due to the difference in the reference frame in which the converter's current is limited. In EMTP, the converter's current is limited in the dq0 frame whereas, for the proposed model, the current is limited in the phase domain. This yields different maximum fault contributions for the two models.

Compared to the current models in CYME 7.0, the proposed model accounts for the overload capability of the converter along with the pre-fault operating conditions and control operating set points as recommended in [25] by the Joint Working Group on Wind Plant Short Circuit Contribution. Besides, no proprietary data is required to model the Type 4 WTG with the proposed model. The only data relative to the converter is its overload design capability which is typically expressed based on the rated power of the WTG. Based on the comparison with CYME current models, the proposed model reproduces better the behavior recommended by the Joint Working Group on Wind Plant Short Circuit Contribution in [25].

As pointed out in [25], proposing a general model of FCG for short-circuit analysis purposes is very difficult as it depends on parameters such as the control strategy implemented which is specific to the WTG manufacturers and the FRT requirements which are specific to either the applicable grid code or the utility. In this respect, the proposed equivalent model of FCG can be considered acceptable as, in most cases, it provides the maximum fault contribution and is therefore on the safe side.

The other contribution of this research work is the development of an iterative fault flow algorithm for the treatment of WTG for short-circuit analysis purposes, based on the Newton MANA method published in [28]. The approach is original as short-circuit algorithms are not iterative by nature. Hence, they are not adapted to accommodate inverter based WTG which behavior is different from traditional generators. The fault-flow algorithm developed provides a simple and yet efficient way of modeling Type 4 WTG thanks to a dynamic Jacobian approach. The performance of the method can be considered acceptable as the algorithm is initialized close to the final solution with a single iteration of the fixed-point method.

This research works sets the groundwork for modeling the Type 4 WTG for short-circuit analysis purposes. However, further work needs to be done to explain the differences with the detailed model in EMTP-RV and to improve the proposed frequency domain model of full converter based wind turbine generators. Besides, it would be interesting to possibly extend the model to other full converter based DG units (micro turbines, photovoltaic panels).

BIBLIOGRAPHIE

1. T. N. Boutsika and S. A. Papathanassiou, *Short-circuit calculations in networks with distributed generation.* Elsevier, 2007: p. 1182 - 1191.
2. *EMTP-RV*. 2011 [On Line]. Available: http://www.emtp.com
3. IEC60909, *Short-circuit currents in three-phase a.c. systems*. 2001.
4. IEEEC37.5, *Guide for Calculation of Fault Currents for Application of AC High-Voltage Circuit Breakers Rated on a Total Current Basis*.
5. L. D. Bellomo, *Comparative Modelling of Wind Parks for Slow and Fast Transients*, in *Electrical Engineering*. 2010, Ecole Polytechnique de Montreal: Montreal.
6. M. Garcia-Sanz, M. Barreras and P. Vital, *Power Regulation Strategies for Wind Turbines*, in *Advances in Wind Energy Conversion Technology*, Springer, Editor. 2011: Berlin. p. 159-176.
7. J. Peralta, S. Dennetière and J. Mahseredjian, *Dynamic Performance of Average-value Models for VSC-HVDC Transmission Systems*, in *Power and Energy Society General Meeting IEEE*. 2012: San Diego, CA. p. 1 - 8.
8. N. Flourentzou, V. G. Agelidis and G. D. Demetriades, *VSC-Based HVDC Power Transmission Systems: An Overview.* Power Electronics, IEEE Transactions **24**(3): p. 592 - 602.
9. M. Valentini, V. Akhmatov, F. Iov and J. Thisted, *Fault Current Contribution from VSC-based Wind Turbines to the Grid.* The Second International Symposium on Electrical and Electronics Engineering, 2008.
10. M. Tsili and S. Papathanassiou, *A review of grid code technical requirements for wind farms.* IET Renewable Power Generation, 2009. **3**(3): p. 308-332.
11. IEEE, *IEEE Application Guide for IEEE Std 1547.2, IEEE Standard for Interconnecting Distributed Resources with Electric Power Systems*. 2008.
12. IEEEC37.010, *IEEE Application Guide for AC High-Voltage Circuit Breakers Rated on a Symmetrical Current Basis.* 1999.
13. N. Samaan, R. Zavadil, J. C. Smith and J. Conto, *Modeling of Wind Power Plants for Short Circuit Analysis in the Transmission Network*, in *Transmission and Distribution Conference and Exposition*. 2008: Chicago, IL. p. 1 - 7.
14. (WWEA), W.W.E.A. *World Wind Energy Association*. February 2012; Available from: http://www.wwindea.org/home/index.php.
15. P. Karaliolios, A. Ishchenko, E. Coster, J. Myrzik and W. Kling, *Overview of Short-Circuit Contribution of Various Distributed Generators on the Distribution Network*, in *Universities Power Engineering Conference, UPEC 2008. 43rd International*. 2008: Padova. p. 1 - 6.

16. T. Ackermann and V. Knyazkin, *Interaction between Distributed Generation and the Distribution Network: Operation Aspects*, in *Transmission and Distribution Conference and Exhibition 2002*. 2002, IEEE/PES: Asia Pacific. p. 1357 - 1362.

17. E. Muljadi, V. Gevorgian, N. Samaan, J. Li and S. Pasupulati, *Short Circuit Current Contribution For Different Wind Turbine Generator Types*, in *Power and Energy Society General Meeting*. 2010, IEEE: Minneapolis, MN. p. 1 - 8.

18. M. E. Baran and I. El-Markaby, *Fault Analysis on Distribution Feeders With Distributed Generators.* IEEE Transactions on Power Systems 2005. **20**: p. 1757-1764.

19. M. Fischer and A. Mendonça, *Representation of Variable Speed Full Conversion Wind Energy Converters for Steady State Short-Circuit Calculations*, in *Power and Energy Society General Meeting, 2011 IEEE*. 2011: San Diego, CA. p. 1 - 7.

20. I. Kocar, J. S. Lacroix and F. Therrien, *General and Simplified Computation of Fault Flow and Contribution of Distributed Sources in Unbalanced Distribution Networks*, in *Power and Energy Society General Meeting*. 2012, IEEE: San Diego, CA. p. 1 - 8.

21. C. A. Plet, M. Graovac, T. C. Green and R. Iravani, *Fault Response of Grid-Connected Inverter Dominated Networks*, in *Power and Energy Society General Meeting*. 2010, IEEE: Minneapolis, MN. p. 1 - 8.

22. R. J. Nelson and H. Ma, *Short-Circuit Contributions of Full-Converter Wind Turbines*, in *Power and Energy Society General Meeting*. 2011, IEEE: San Diego, CA. p. 1 - 4.

23. D. Turcotte and F. Katiraei, *Fault Contribution of Grid-Connected Inverters*, in *Electrical Power & Energy Conference (EPEC)*. 2009, IEEE: Montreal, QC. p. 1 - 5.

24. R. A. Walling and M. L. Reichard, *Short Circuit Behavior of Wind Turbine Generators*, in *Protective Relay Engineers, 2009 62nd Annual Conference*. 2009: Austin, TX. p. 492 - 502.

25. R. Walling, R. Harley, D. Miller and G. Henneberg, *Fault Current Contributions from Wind Plants*.

26. R. A. Walling, E. Gursoy and B. English, *Current Contributions from Type 3 and Type 4 Wind Turbine Generators During Faults*, in *PES General Meeting*. 2011: Detroit, MI.

27. A. Yazdani and R. Iravani, *A Unified Dynamic Model and Control for the Voltage-Sourced Converter Under Unbalanced Grid Conditions.* IEEE Transactions on Power Delivery, 2006. **21**(3): p. 1620-1629.

28. I. Kocar, J. Mahseredjian, U. Karaagac, G. Soykan and O. Saad, *Multiphase Load-Flow Solution for Large Scale Distribution Systems using MANA.* Power Delivery, IEEE Transactions, 2013. **PP**(99): p. 1.

29. A. Gueye, *CYME 7.1 Load-Flow MANA Solver*. 2013.

30. M. Z. Kamh and R. Iravani, *A Unified Three-Phase Power-Flow Analysis Model For Electronically-Coupled Distributed Energy Resources.* Power Delivery, IEEE Transactions, 2011. **26**(2): p. 899 - 909.

31. M. Valentini, *Fault Current Contribution from VSC-based Wind Turbines to the Grid*, in *Institute of Energy Technology*. 2008, Aalborg University: Denmark. p. 134.

32. TransEnergie, H.Q., *Transmission Provider Technical Requirement For the Connection of Power Plants To The Connection of Power Plants To The Hydro-Quebec Transmission System*. 2009.

33. J. S. Lacroix, *Multiphase Short-Circuit Analysis Solver In Phase Domain Using A Modified-Augmented-Nodal Analysis Approach*. 2012, Ecole Polytechnique: Montréal.

34. R. C. Dugan, *A Perspective On Transformer Modeling for Distribution Svstem Analvsis*, in *Power Engineering Society General Meeting*. 2003. p. 114-119.

35. J. Peralta, F. de León and J. Mahseredjian, *Assessment of Errors Introduced by Common Assumptions Made in Power System Studies*, in *Power and Energy Society General Meeting*. 2011: San Diego, CA. p. 1-8.

36. S. Bernard, D. Beaulieu and G. Trudel, *Hydro-Québec grid code for wind farm interconnection, in Power*

Engineering Society General Meeting. 2005, IEEE. p. 1248 - 1252.

37. Gmbh, E.O.N., *Grid code - high and extra high voltage*. 2006: Bayreuth, Germany

38. 32.0, P., *PSSE Program Operation Manual*, June 2009

39. REE, *Requisitos de repuesta frente a huecos de tension de las instalaciones de*

produccion de regimen especial, November 2005, Spain

40. I. Erlich, W. Winter and A. Dittrich, *Advanced Grid Requirements for the Integration of Wind Turbines into the German Transmission System*. IEEE Power Engineering Society General Meeting 2006.

41. CYME Software, 2013 [On Line]. Available: http://www.cyme.com

42. CYMSTAB Software, 2013 [On Line]. Available: http://www.cyme.com

43. Wind Turbine Blade Aerodynamics, [Online]. Available: http://www.gurit.com/files/documents/2_aerodynamics.pdf

44. J. Mahseredjian, S. Dennetière, L. Dubé, B. Khodabakhchian and L. Gérin-Lajoie, *On a new approach for the simulation of transients in power systems*, in *6th International Conference on Power System Transients*, 2007, p. 1514-1520.

APPENDIX 1 – DATA FOR THE FORTIS ALBERTA 25 KV SYSTEM

The system data is presented in the following tables:

Table I: Substation data

Bus	X_0 [ohms]	R0 [ohms]	X_{1sub} [ohms]	R_{1sub} [ohms]	X_2 [p.u.]	R_2 [p.u.]
GLENWOOD_B1	43.82948	5.0115	15.5336	9.69638	9.69638	15.5336

Table II: Cable data

Cable Id	X_0 [Ω /km]	R_0 [Ω /km]	X_1 [Ω /km]	R_1 [Ω /km]	B_0 [μS/km]	B_1 [μS /km]	Length [km]
L1	1.9167	0.513	0.4294	0.3393	1.576	4.0301	4.6
L10	1.9167	0.513	2.0395	1.2733	1.576	0.0	1.0
L2	1.9167	0.513	0.4294	0.3393	1.576	4.0301	16.7
L3	1.9167	0.513	0.4294	0.3393	1.576	4.0301	4.6
L4	1.9167	0.513	0.4294	0.3393	1.576	4.0301	10.6
L5	1.9167	0.513	0.4294	0.3393	1.576	4.0301	6.8
L6	1.9167	0.513	0.4294	0.3393	1.576	4.0301	5.0
L7	1.9167	0.513	0.4294	0.3393	1.576	4.0301	14.2
L8	1.9167	0.513	0.4294	0.3393	1.576	4.0301	9.7
L9	1.9167	0.513	0.4294	0.3393	1.576	4.0301	2.5
L8	1.9167	0.513	0.4294	0.3393	1.576	4.0301	150

Table III: Transformer data

Low Voltage Bus	**High Voltage Bus**	**Z_1 [p.u.]**	**Z_0 [p.u.]**	**X_1/R_1**	**X_0/R_0**	**Primary Voltage [kV]**	**Secondary Voltage [kV]**	**Nominal Rating [kVA]**
147-0	BUS_G	5.8	5.8	42	42	25	0.24	750
FROM_BUS_R3	BUS_H	0.12	0.12	999	999	25	25	13000
TO_BUS_R2	BUS_D	0.12	0.12	999	999	25	25	13000
BUS_C	SOURCE	7.0	7.0	13.0	13.0	69	25	12000
FROM_BUS_R1	TO_BUS_R1	0.12	0.12	999	999	25	25	13000